Progress in Nuclear Magnetic Resonance Spectroscopy 55 (2009) 215–237

Contents lists available at ScienceDirect

Progress in Nuclear Magnetic Resonance Spectroscopy

journal homepage: www.elsevier.com/locate/pnmrs

Solid-state NMR of quadrupolar halogen nuclei

Rebecca P. Chapman, Cory M. Widdifield, David L. Bryce *

Department of Chemistry and Centre for Catalysis Research and Innovation, University of Ottawa, Ottawa, Ont., Canada K1N6N5

ARTICLE INFO

Article history:
Received 31 March 2009
Accepted 5 May 2009
Available online 15 May 2009

Keywords:
Chlorine
Bromine
Iodine
Chemical shift
Quadrupolar coupling constant
Nuclear magnetic resonance
NMR
Tensors

Contents

Abbreviations: Cp, cyclopentadienyl; Cp*, pentamethylcyclopentadienyl; CP/MAS, cross-polarization magic-angle spinning; C_Q, quadrupolar coupling constant; CS, chemical shift; CSA, chemical shift anisotropy; CT, central transition; δ_{11}, δ_{22}, δ_{33}, principal components of the chemical shift tensor; EFG, electric field gradient; η_Q, quadrupolar asymmetry parameter; HMS, Haeberlen–Mehring–Spiess; IUPAC, International union of pure and applied chemistry; κ, skew of the magnetic shielding (or chemical shift) tensor; MAS, magic-angle spinning; MQMAS, multiple-quantum magic-angle spinning; NQR, nuclear quadrupole resonance; PAS, principal axis system; Q, nuclear electric quadrupole moment; QCPMG, quadrupolar Carr–Purcell–Meiboom–Gill.

* Corresponding author. Tel.: +1 613 562 5800x2018; fax: +1 613 562 5170.
E-mail address: dbryce@uottawa.ca (D.L. Bryce).

doi:10.1016/j.pnmrs.2009.05.001

1. Introduction

Chlorine, bromine, and iodine are elements of importance in a variety of inorganic and organic compounds. For example, chlorine plays an important biological role in vital chloride ion channels [1–4] and all three elements are present in a variety of inorganic catalysts [5,6]. Solid-state nuclear magnetic resonance (SSNMR) spectroscopy of the chlorine-35/37, bromine-79/81, and iodine-127 nuclides is often challenging due to their NMR properties; however, the experiment is an excellent probe of the local halogen environment in many solid compounds and materials because of the technique's sensitivity to the local electronic and structural environments.

Chlorine-35/37 ($I = 3/2$), bromine-79/81 ($I = 3/2$), and iodine-127 ($I = 5/2$) are all NMR-active quadrupolar nuclei that are present in relatively high natural abundances (Table 1). As these nuclei are quadrupoles, the collection of high signal-to-noise (S/N) ratio SSNMR spectra may be difficult, especially for powder samples. In systems where the nucleus does not sit at a site of very high symmetry (e.g., octahedral or tetrahedral), the interaction between the quadrupole moment (Q) of the nucleus and the electric field gradient (EFG) tensor is a significant perturbing interaction to the Zeeman Hamiltonian, which broadens the resulting NMR spectrum of a powder. As halogen atoms do not generally sit at a site of high symmetry in the majority of systems of interest, quadrupolar broadening is generally the dominant contribution to the observed NMR line widths. In these cases, often only the central transition (CT, $m = ½ \leftrightarrow -½$) is observed; even this may be broadened to a significant extent, up to the order of magnitude of MHz in some cases. Further discussion of the NMR properties of the quadrupolar halogen nuclei is given in Section 2.3. Despite the challenges, there have been a number of significant studies using chlorine, bromine,

Table 1
NMR properties of the quadrupolar halogens (chlorine, bromine, and iodine).

	Natural abundance/%	I	$\gamma/10^7$ rad T^{-1} s^{-1}	Ξ[a]	Q/mb	$1-\gamma_\infty$[17]	Relative CT line width[b]	IUPAC chemical shift reference[c]
^{35}Cl	75.78	3/2	2.624198	9.797909	−81.65(80)	42.0	1.34	0.1 mol/dm^3 NaCl in D_2O
^{37}Cl	24.22	3/2	2.184368	8.155725	−64.35(64)	42.0	1.00	
^{79}Br	50.69	3/2	6.725616	25.05390	313(3)	80	7.70	0.01 mol/dm^3 NaBr in D_2O
^{81}Br	49.31	3/2	7.249776	27.00658	262(3)	80	5.01	
^{127}I	100.0	5/2	5.389573	20.00748	−696(12)	162	11.44	0.01 mol/dm^3 KI in D_2O

[a] Resonance frequency, in MHz, in a magnetic field where ^{1}H resonates at exactly 100 MHz.
[b] For a powder sample, based on Eq. (13).
[c] From reference [177].

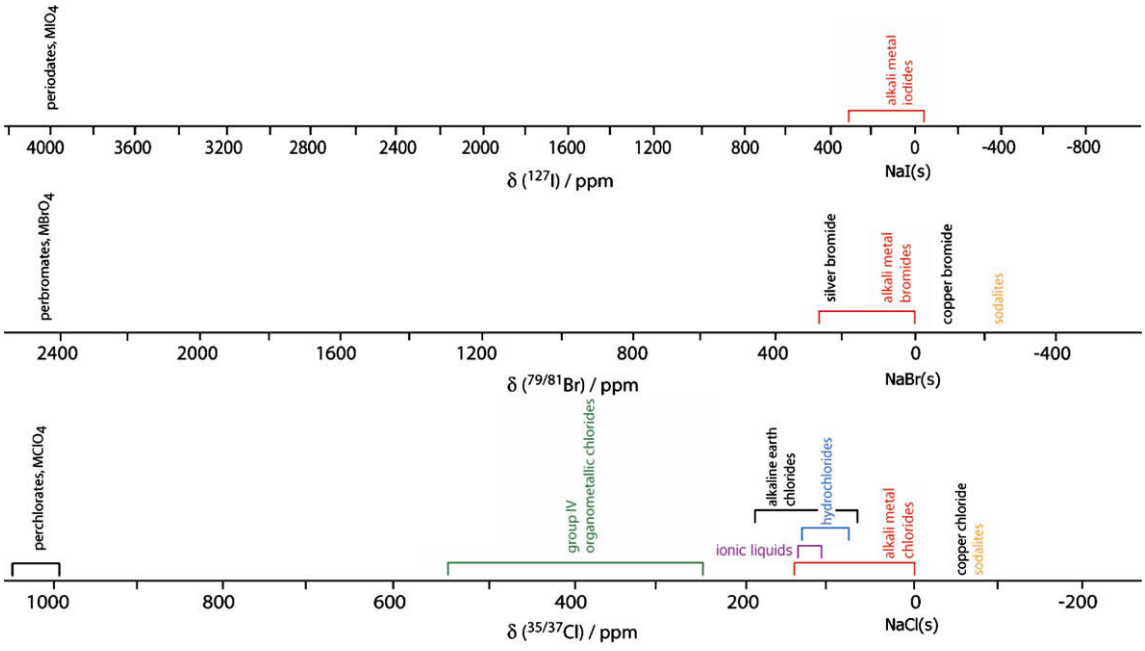

Fig. 1. Approximate chemical shift ranges for chlorine, bromine, and iodine. Scales are with respect to solid NaX (X = Cl, Br, and I) at 0 ppm. Note the different scale for each element.

and iodine SSNMR, and with the availability of high (and ultrahigh, $\geqslant$18.8 T) magnetic fields, the amount of research occurring in this area is expected to grow. Presented in Fig. 1 are the approximate solid-state chemical shift ranges for $^{35/37}$Cl, $^{79/81}$Br, and ^{127}I in various types of compounds. It is apparent that the majority of studies have been performed on halides and perhalogenates, due to the high symmetry (and corresponding small or negligible EFG) at the halogen nuclei in these compounds.

This article is a concise overview of chlorine, bromine, and iodine SSNMR, discussing the experimental data from selected studies of diamagnetic samples, with emphasis on the most recent advancements in the field. Two reviews of chlorine-35/37, bromine-79/81, and iodine-127 SSNMR have previously been published. The first surveys the literature up to July 2005 [7], while the second provides a comprehensive examination of this field, up to August 2008 [8]. There have also been reviews of solution-state chlorine, bromine, and iodine NMR by Lindman and Forsén in 1976 [9] and 1978 [10], Forsén and Drakenberg in 1983 [11] and Akitt in 1987 [12].

We emphasize that quadrupolar interaction (QI) data for $^{79/81}$Br and ^{127}I in particular are available for a wide range of compounds, primarily via NQR spectroscopy and Zeeman-perturbed NQR experiments. We refer the reader to Lucken's monograph [13] and to our most recent prior review [8] for more comprehensive accounts of the data obtained from these techniques.

2. Theory, conventions, and chemical shift referencing

The Hamiltonian operator ($\hat{H}$) for a NMR-active nucleus within a solid sample contains a term arising from the nuclear magnetic shielding ($\hat{H}_\sigma$) interaction, which acts as a perturbation to the Zeeman term ($\hat{H}_Z$). The latter term arises from the interaction of the nuclear magnetic moment with the external applied magnetic field, B_0. In the case of the quadrupolar chlorine, bromine, and iodine nuclides, the Hamiltonian contains a quadrupolar term as well ($\hat{H}_Q$). There are other terms, e.g., direct homonuclear and heteronuclear dipolar coupling, as well as indirect (J) spin–spin coupling, which may be present, but these have a negligible impact on the chlorine, bromine, and iodine SSNMR spectra for most of the compounds studied to date. Thus, only the nuclear magnetic shielding and QI will be briefly described below for the case of diamagnetic powders. More complete theoretical treatments are available and for these the reader is referred elsewhere [13–19].

2.1. Magnetic shielding interaction and chemical shifts

In powdered solids, the averaging of the magnetic shielding tensor (σ) that occurs in liquids, due to rapid, isotropic molecular tumbling, is absent and therefore the shielding is not averaged to its isotropic value (σ_{iso}). In the absence of magic-angle spinning (MAS), the shielding arising from all molecular orientations in a powdered sample contribute to the SSNMR spectrum to produce an anisotropic 'powder pattern'. While it is not generally possible to measure shielding constants directly in conventional NMR experiments, it is routine to measure the shielding difference between two compounds, with one serving as a reference. This "chemical" shift (CS, δ) can be defined in terms of magnetic shielding as:

$$\delta = \frac{\sigma_{ref} - \sigma}{1 - \sigma_{ref}}, \tag{1}$$

where σ and σ_{ref} represent the magnetic shielding of the sample and the reference, respectively. The CS may be more practically defined in terms of resonance frequencies in lieu of shielding constants:

$$\delta = \frac{\nu - \nu_{ref}}{\nu_{ref}}. \tag{2}$$

In Eq. (2), ν and ν_{ref} represent the resonance frequency of the sample and the reference (in the same B_0), respectively.

Both the magnetic shielding and CS are second-rank tensor quantities which, when diagonalized, have three principal components (i.e., eigenvalues) associated with their principal axis system (PAS; i.e., eigenvectors). Thus, Eq. (1) may be used to calculate each element of a chemical shift tensor (δ_{ij}), from the corresponding magnetic shielding tensor element (σ_{ij}) of the sample, if the isotropic magnetic shielding value of the reference is also known. The principal components of the chemical shift tensor are defined such that $\delta_{11} \geqslant \delta_{22} \geqslant \delta_{33}$.

The convention for reporting chemical shift anisotropy (CSA) data is not uniform within the literature. Popular conventions include the Haeberlen–Mehring–Spiess [20–23] convention and the Herzfeld–Berger/Maryland convention [21,24]. A brief summary of both conventions is therefore warranted. Where we have summarized CS tensor data in this article, we have reported the principal components, when possible.

2.1.1. Haeberlen–Mehring–Spiess (HMS) convention

There are three parameters in the HMS convention that are defined in terms of the three shielding tensor principal components: σ_{XX}, σ_{YY}, and σ_{ZZ}. These parameters are the isotropic shielding value (σ_{iso}), the shielding tensor anisotropy ($\Delta\sigma$), and the shielding tensor asymmetry (η), which are defined below:

$$\sigma_{iso} = \frac{\sigma_{XX} + \sigma_{YY} + \sigma_{ZZ}}{3} \tag{3}$$

$$\Delta\sigma = \sigma_{ZZ} - \frac{(\sigma_{XX} + \sigma_{YY})}{2} \tag{4}$$

$$\eta = \frac{3(\sigma_{YY} - \sigma_{XX})}{2\Delta\sigma} \tag{5}$$

where $|\sigma_{ZZ} - \sigma_{iso}| \geqslant |\sigma_{XX} - \sigma_{iso}| \geqslant |\sigma_{YY} - \sigma_{iso}|$. The sign of $\Delta\sigma$ therefore depends on the size of σ_{ZZ} relative to σ_{iso}, and is positive if $\sigma_{ZZ} > \sigma_{iso}$ and negative if $\sigma_{ZZ} < \sigma_{iso}$. This fact can complicate the comparison of $\Delta\sigma$ values across a range of compounds. The asymmetry is always positive, taking a value between 0 and 1.

2.1.2. Herzfeld–Berger/Maryland convention

The three principal components of the shielding tensor, σ_{11}, σ_{22}, and σ_{33}, are always arranged as follows: $\sigma_{11} \leqslant \sigma_{22} \leqslant \sigma_{33}$. As in the HMS convention, the isotropic shielding value is the average of the three principal components: $(1/3)(\sigma_{11} + \sigma_{22} + \sigma_{33})$. The other parameters used to describe the magnetic shielding tensor are the span (Ω), which describes the breadth of the pattern, and the skew (κ), which describes the asymmetry. These parameters are defined below:

$$\Omega = \sigma_{33} - \sigma_{11}; \tag{6}$$

$$\kappa = \frac{3(\sigma_{iso} - \sigma_{22})}{\Omega}. \tag{7}$$

The span can take on any positive value, while the skew ranges between −1 and +1. One advantage of the Herzfeld–Berger/Maryland convention is the direct comparison between the CS and the magnetic shielding tensor. The definitions of the three parameters can be applied to the CS tensor, as shown below:

$$\delta_{iso} = \frac{\delta_{11} + \delta_{22} + \delta_{33}}{3}; \tag{8}$$

$$\Omega \approx \delta_{11} - \delta_{33}; \tag{9}$$

$$\kappa = \frac{3(\delta_{22} - \delta_{iso})}{\Omega}. \tag{10}$$

As long as $1-\sigma_{ref}$ is close to unity, Eq. (9) is valid, allowing for the direct comparison of chemical shift and (often calculated) magnetic

shielding data. This is practically always the case when discussing chlorine, bromine, and iodine SSNMR data.

2.2. Nuclear electric quadrupolar interaction

As chlorine, bromine, and iodine are all quadrupolar nuclei, the nuclear charge is distributed asymmetrically about the nucleus. The resultant Q will couple with the EFG tensor ($\boldsymbol{V}$) at the nuclear centre. The EFG tensor is traceless and symmetric and may be described by five independent parameters. In its PAS, the three principal components of the tensor are labelled, V_{11}, V_{22}, and V_{33}, with magnitudes arranged as shown:

$$|V_{33}| \geq |V_{22}| \geq |V_{11}|.$$

Three Euler angles describe the orientation of the EFG PAS with respect to an external axis system. Since the EFG tensor is traceless, the principal components may be fully described using two independent parameters. These components are generally expressed in terms of the quadrupolar coupling constant (C_Q) and the asymmetry parameter (η_Q):

$$C_Q = \frac{eV_{33}Q}{h}; \tag{11}$$

$$\eta_Q = \frac{V_{11} - V_{22}}{V_{33}}, \tag{12}$$

where h is Planck's constant and e is the elementary charge. The quadrupole moment is a constant for a given nucleus (Table 1).

To fully describe the CS and EFG tensors, the orientations of their PASs must be known. In practice, for powder samples one typically measures the relative orientation of the PASs of the CS and EFG tensors. This requires an additional three parameters, known as the Euler angles, α, β, and γ. Under the Arfken convention [25], these angles describe the counter-clockwise rotations of the CS tensor away from the stationary EFG reference tensor, assuming initial coincidence of the two PASs. Specifically, α describes the initial rotation about the original δ_{33} axis, β is a rotation about the new direction of δ_{22}, and γ is the final rotation, around the new direction of δ_{33}, as shown in Fig. 2.

Chlorine, bromine, and iodine all have moderate to high Q values and thus the quadrupolar interaction is often quite significant. Hence, first-order perturbation theory generally fails to describe the SSNMR line shapes which are observed experimentally for powdered samples. However, second-order perturbation theory

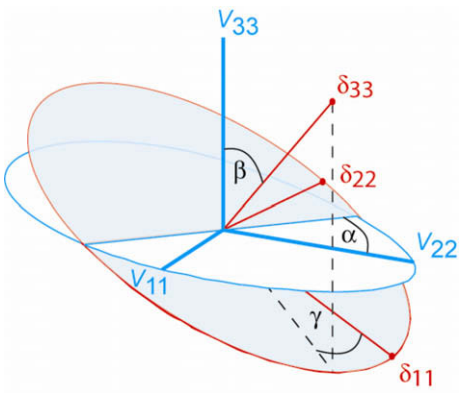

Fig. 2. Depiction of the Euler angles α, β, and γ used for relating the principal axis systems (PASs) of the electric field gradient tensor ($\boldsymbol{V}$) and the chemical shift tensor ($\boldsymbol{\delta}$). The angles may also be visualized as counterclockwise rotations of the $\boldsymbol{\delta}$ tensor PAS away from the $\boldsymbol{V}$ PAS: first about the eigenvector corresponding to δ_{33} through an angle α, then about the intermediate direction of the δ_{22} eigenvector by an angle β, then about the final direction of the δ_{33} eigenvector by an angle γ.

usually adequately describes the experimental SSNMR line shape. Generally in the case of these nuclei, the QI is sufficiently large to broaden the satellite transitions (ST) to such an extent that they cannot be observed, and experimentally only the CT can be detected. The CT is not broadened by first order quadrupolar effects but is affected in the second order. The breadth of the CT line shape of a stationary powdered sample depends on four parameters (C_Q, ν_0, I, and η_Q), as shown below [17]:

$$\Delta\nu_{CT} = \left[\frac{3C_Q}{2I(2I-1)}\right]^2 \frac{(\eta_Q^2 + 22\eta_Q + 25)(I(I+1) - \frac{3}{4})}{144\nu_0}, \tag{13}$$

where ν_0 is the Larmor frequency. The inverse proportionality between $\Delta\nu_{CT}$ and ν_0 demonstrates why higher magnetic fields are advantageous for the quadrupolar halogens: increasing B_0 increases ν_0, and therefore results in a decrease in the second-order quadrupolar broadening of the CT. Presented in Table 1 are the relative values of $\Delta\nu_{CT}$ for the five quadrupolar halogen nuclides for a given EFG; these are calculated directly from Eq. (13). It is also worth noting that the effects of CSA increase at higher fields, allowing for these effects to be more easily observed in cases where there is a significant QI. In addition, for a given EFG tensor, narrower CT powder patterns are obtained for higher half-integer spin nuclei (see Eq. (13)).

The Sternheimer antishielding factor, $1-\gamma_\infty$, modifies the EFG 'felt' at the nucleus due to the polarization of inner-shell electrons [13,26,27]. That is, the EFG due solely to ionic charges in the lattice, eq_{ionic}, is modified as follows [28]:

$$eq_{observed} = (1 - \gamma_\infty)eq_{ionic}. \tag{14}$$

The quantity $eq_{observed}$ must be considered for the accurate discussion of quadrupolar coupling constants and relative line widths (*vide supra*). The antishielding factors for Cl, Br, and I are tabulated in Table 1. Wu and Terskikh have recently demonstrated the importance of considering the antishielding factors when comparing NMR data for alkali metal cations in isostructural tetraphenylborate salts [28]. The importance for chlorine, bromine, and iodine may also be seen by considering that $1-\gamma_\infty$ increases from 42.0 to 80 to 162 for these three elements. We may appreciate the impact of antishielding by considering the following: assuming each of the nuclides in turn is hypothetically placed into the same crystal lattice of fixed geometry and volume, they will experience identical electric field gradients due to the charges in the lattice (eq_{ionic}). However, the EFG at the nucleus will differ due to the different values of the antishielding factors, as per Eq. (14). The relative impact due to antishielding on the value of $\Delta\nu_{CT}$ may be assessed by evaluating $[Q(1-\gamma_\infty)]^2/\gamma$. The results for an axially symmetric EFG are 44.8, 33.4, 930, 610, and 23600 $\times 10^{-64}$ m^4 rad^{-1} T s for ^{35}Cl, ^{37}Cl, ^{79}Br, ^{81}Br, and ^{127}I, respectively. This highlights the challenge of observing ^{127}I NMR spectra even in chemical environments where chlorine and bromine NMR spectra have been successfully acquired. Of course, the above assessment does not take into account the nuclear spin quantum numbers, which also affect the line widths, according to Eq. (13).

For the majority of the results discussed in this work, the high-field approximation, which assumes that ν_0 is much greater than the quadrupolar frequency (ν_Q),

$$\nu_Q = \frac{3C_Q\sqrt{1 + \frac{\eta_Q^2}{3}}}{2I(2I-1)} \tag{15}$$

is used. The validity of this approximation in the case of nuclei with large quadrupole moments depends on the EFG tensor at the nuclear site in a given compound; the value of ν_Q may become comparable to the Larmor frequency in certain cases. The range of validity was recently tested through several simulations that highlighted the differences between the second-order and exact approaches

[8,29]. It was found that the difference between the calculated exact and second-order perturbation theory CT resonance frequencies for a single crystal is negligible (<1%) for practical purposes up until the point where ν_Q is $\nu_0/2$ for $I = 3/2$, and $\nu_0/5$ for $I = 5/2$. The difference is even smaller in the case of the CT of a powdered sample. These results suggest that the common rule-of-thumb regarding the validity of the second-order approximation (i.e., $\nu_Q < 0.1\nu_0$) may be slightly conservative, particularly for powdered samples [8].

2.3. NMR properties of chlorine, bromine, and iodine

Of the quadrupolar halogens, chlorine is the most "NMR friendly", with its two NMR-active isotopes having quadrupole moments significantly lower than those of both bromine and iodine (Table 1). Although the quadrupole moment of ^{37}Cl is lower, ^{35}Cl is the more commonly studied isotope due to its higher natural abundance. The moderately low Larmor frequencies of ^{35}Cl and ^{37}Cl can present some problems with acoustic ringing in low magnetic fields, but with the increased availability of higher field instruments, chlorine experiments are becoming more accessible. ^{35}Cl resonates just below ^{15}N and so it is often possible to observe ^{35}Cl on a standard HCN probe. Compared to chlorine, $^{79/81}$Br and ^{127}I have higher Larmor frequencies and their NMR-active isotopes exist in high natural abundances; however, their moderately large quadrupole moments and the concomitant spectral broadening make collecting spectra of these nuclei difficult, except in cases of very high symmetry. Of the three halogens, ^{127}I is generally the most difficult nucleus to study experimentally, despite its 100% natural abundance, higher value of I, and moderate ν_0, due to its large Q value and the typical electronic environments in which ^{127}I is found.

Solution-state NMR standards for each of the three nuclei have been recommended [30], as shown in Table 1. When using these standards, the concentration must be carefully determined and noted as the chemical shift may vary with concentration [31]. The solvent (e.g., H_2O vs D_2O) is even more important, as significant isotope effects are known to exist [7,32]. For example, for a 1–3 M NaCl solution, $\delta(^{35}Cl, H_2O)-\delta(^{35}Cl, D_2O) = 4.7 \pm 0.3$ ppm; for a 0.41–0.82 M RbBr solution, $\delta(^{79/81}Br, H_2O)-\delta(^{79/81}Br, D_2O) = 8.3 \pm 0.3$ ppm and for a 0.45–0.95 M NaI solution, $\delta(^{127}I, H_2O)-\delta(^{127}I, D_2O) = 13.2 \pm 2.5$ ppm [33]. The alternative references of solid NaCl or KCl have been suggested for $^{35/37}$Cl, and solid KBr for $^{79/81}$Br, as they produce narrow lines at relatively slow spinning speeds because of their cubic structures. In addition, this removes any ambiguity in terms of concentration or solvent isotope effects [7,8].

To facilitate chemical shift referencing using solid powdered alkali metal halides, we have measured their chemical shifts with respect to the IUPAC standards (Table 2). Shown in Figs. 3 and 4 are chlorine-35/37 and iodine-127 SSNMR spectra of solid powdered alkali metal halides with respect to the solution-state IUPAC standards. The ^{79}Br and ^{81}Br chemical shifts of the alkali metal bromide salts, relative to the IUPAC solution standard, were reported by Widdifield et al. [8] All the data are presented in Table 2.

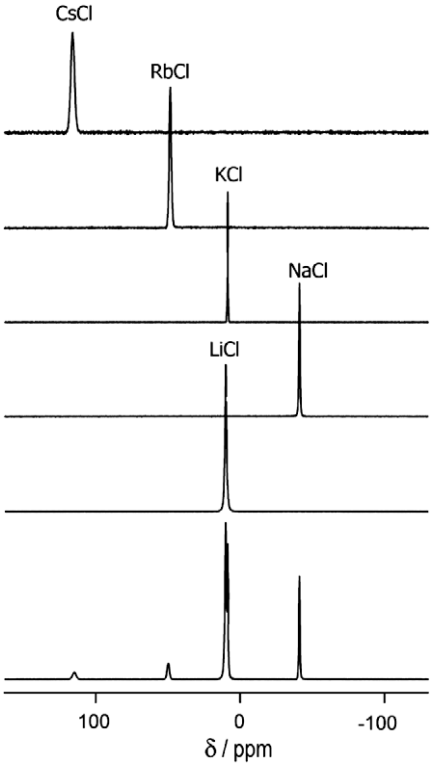

Fig. 3. Chlorine-35 MAS NMR spectra of powdered alkali metal chlorides ($B_0 = 9.4$ T). Spectra of the individual samples are shown in the top traces, with the centrebands labelled. Spectrum of a mixture of the five compounds is also shown (bottom). The chemical shifts are referenced with respect to the IUPAC standard, 0.1 mol dm^{-3} NaCl in D_2O at 0 ppm. (see Table 2 for chemical shifts).

Of the nuclei under discussion, chlorine is the only one for which a precise absolute shielding scale is available. This scale was determined through a combined experimental and theoretical study. An isotropic magnetic shielding constant (σ_{iso}) of 974(4) ppm was determined for a chloride ion in an infinitely dilute aqueous solution [34]. The conversion between shielding and shift is therefore as follows (cf. Eq.(1)):

$$\delta = (974\text{ppm} - \sigma)/(1 - 974\text{ppm}) \quad (16)$$

and is an improvement over prior chlorine absolute shielding scales [35,36].

The bromine and iodine absolute shielding scales are much less precisely determined and in fact no references have been made to

Table 2
Solid-state halogen isotropic chemical shifts of the alkali metal halides, MX.[a]

	With respect to KX(*s*)			With respect to IUPAC aqueous standard			
	M^{35}Cl[b]	M^{79}Br[b]	M^{127}I[b]	M^{35}Cl[c]	M^{79}Br[d]	M^{81}Br[d]	M^{127}I[e]
LiX	1.31	64.74	215.28	9.93	119.06	119.33	408.66
NaX	−49.73	−52.89	33.53	−41.11	1.29	1.57	226.71
KX	0	0	0	8.54	54.31	54.51	192.62
RbX	41.13	71.66	76.91	49.66	125.89	126.13	269.87
CsX	105.96	227.43	368.69	114.68	282.66	282.76	562.41

[a] Slight differences (<1 ppm) between relative shifts with respect to the solid and the solution are seen; this is likely due to the fact that the data come from two different sources.
[b] With respect to KX(*s*). From references [69,74].
[c] With respect to 0.1 M NaCl in D_2O.
[d] With respect to 0.03 M NaBr in D_2O. From reference [8].
[e] With respect to 0.01 M KI in D_2O.

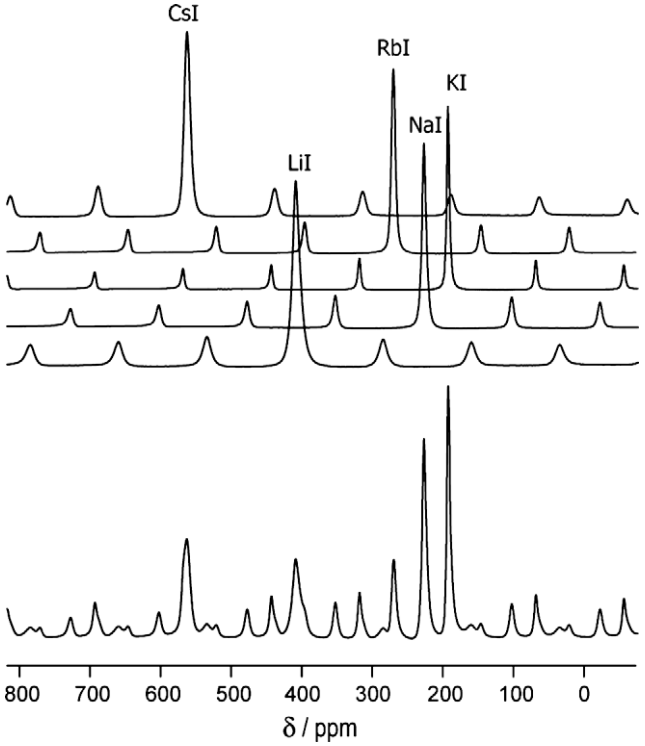

Fig. 4. Iodine-127 MAS NMR spectra of powdered alkali metal iodides (B_0 = 9.4 T). Spectra of the individual samples are shown in the top traces, with the centreband labelled. A spectrum of a mixture of the five compounds is also shown (bottom). The chemical shifts are referenced with respect to the IUPAC standard, 0.01 mol dm^{-3} KI in D_2O at 0 ppm (see Table 2 for chemical shifts).

the bare nuclei. Hartree–Fock methods using a semi-quantitative theoretical model [37] in combination with experimental data [38,39] were used to calculate the shift of the bromide anion in dilute aqueous solution with respect to the free gas-phase anion as −194 ppm [40]. For I^- in dilute aqueous solutions, a value of −600 ppm with respect to the free anion was determined by Itoh and Yamagata via experimental solution-state measurements [41]. It is non-trivial to establish a reliable absolute shielding scale for bromine and iodine, as it is not clear how the non-relativistic relationship between the spin-rotation tensor and the magnetic shielding tensor (which is a common method of establishing an absolute shielding scale for a particular nuclide) is affected when relativistic effects become important [42,43].

3. Experimental methods for powders

3.1. Magic-angle spinning and stationary samples

The majority of SSNMR studies on chlorine, bromine, and iodine are done on powdered samples. With powdered samples, MAS experiments are a powerful method of study in cases when the broadening of the CT is small enough to allow for the acquisition of a MAS NMR spectrum with resolution of spinning sidebands (ssb) from the centreband. In these cases, the resultant centreband line shape is free of any CSA effects. The second-order QI is not completely averaged by the spinning, thereby allowing for the extraction of C_Q and η_Q, along with δ_{iso}, as these are the three parameters that quantify the line shape and position of the centreband.

As the broadening associated with the QI decreases with increasing field (Eq. (13)), the increased availability of high/ultra-high–field magnets has allowed for the acquisition of MAS spectra for materials with a greater range of C_Q values. In addition, advances in probe technology allow for higher spinning rates and have also opened the door to studying a variety of materials with more strongly quadrupolar-broadened NMR lineshapes. Currently, the highest magnetic field readily available for SSNMR studies is 21.84 T and the highest commercially available MAS frequency is ~70 kHz, using a 1.3 mm o.d. rotor.

Two-dimensional (2D) NMR experiments have been developed to collect high-resolution "isotropic" spectra of half-integer quadrupolar nuclei in which the quadrupolar effects have been removed from the MAS spectrum. These include the multiple-quantum MAS (MQMAS) and satellite transition MAS (STMAS) pulse sequences. Both 2D sequences remove the quadrupolar broadening in one dimension through excitation of either multiple-quantum coherences (in MQMAS)[44] or satellite transitions (in STMAS) [45], followed by a transfer of the magnetization to the CT for detection and appropriate data processing. To the best of our knowledge, the STMAS experiment has not been applied to chlorine, bromine, or iodine. There exists one example of MQMAS applied to the quadrupolar halogens: Trill et al. report the collection of a ^{35}Cl MQMAS spectrum in their study of chlorine-containing sodalites, although the spectrum is not shown in their publication [46]. While both pulse sequences are very useful for a variety of nuclei, it appears that their application to the quadrupolar halogens is hindered due to the large QI in many of the materials of interest.

A common experimental technique used to improve the quality of the CT spectrum for the quadrupolar halogens is a simple quadrupolar echo. Due to the large Q values for the quadrupolar halogens, the line shapes in the resulting spectra are often very broad and therefore have rapidly decaying free induction decays (FIDs). With chlorine, this may be coupled with the presence of acoustic ringing in the coil, which can prevent the measurement of the resulting signal. This problem is remedied by a quadrupolar echo, as it shifts the FID forwards in the time domain. The quadrupolar Carr–Purcell–Meiboom–Gill (QCPMG) pulse sequence [47] is also used to improve experimental sensitivity and has started to be applied to chlorine and bromine [48–53]. The experiment consists of the collection of the FID after each pulse in a train of refocusing π pulses after an initial $\pi/2$ pulse. After Fourier transformation, the frequency-domain spectrum is a powder pattern which is split into "spikelets". The experiment can be carried out under stationary, MAS, and MQMAS conditions and improves experimental sensitivity on two fronts: firstly, the multiple signal acquisition periods per relaxation delay and secondly, the enhancement from concentrating the total signal intensity into the spikelets. The improved sensitivity greatly reduces the acquisition time needed to collect a spectrum with adequate S/N, compared to a spin echo. Siegel et al. used the QCPMG experiment to acquire a ^{127}I NMR spectrum of KIO_4, a compound which has a C_Q value over 20 MHz (Fig. 5) [54]. We have found this compound to be an excellent set-up sample for ^{127}I QCPMG NMR experiments.

Other signal enhancement methods are available to increase the S/N ratio of the spectrum of the CT. A popular approach is to 'borrow' intensity from the satellite transitions either through saturation or inversion of their populations [55]. Implementations of these methods, such as double-frequency sweeps (DFS)[56] and hyperbolic secant pulses [57], have begun to be applied to the quadrupolar halogens, and they will likely prove useful in future experiments. For example, Bryce et al. have reported applications of the hyperbolic secant enhancement method for ^{35}Cl NMR studies of amino acid hydrochlorides [49].

In some instances, the line width of the central transition is so large that it is not possible for it to be uniformly excited. In this case, variable-offset experiments are useful to collect the full SSNMR spectrum. The approach of these experiments is simple: the rf transmitter is systematically stepped across the entire

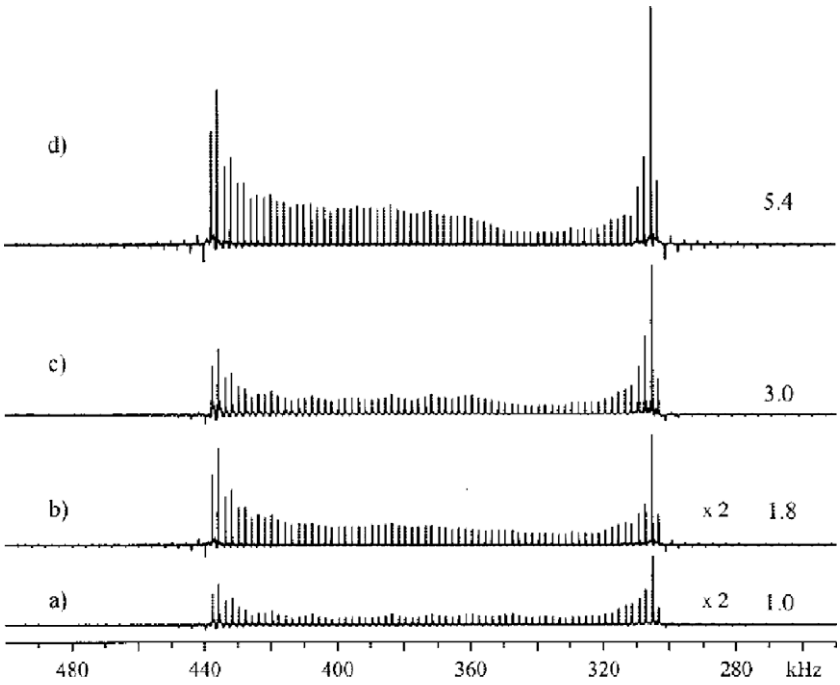

Fig. 5. Iodine-127 NMR spectra of solid powdered KIO_4 obtained under stationary conditions at 11.75 T. Pulse sequence used: (a) QCPMG; (b) modified QCPMG (the repeating π pulses are replaced with $\pi/2$ pulses); (c) converging DFS with QCPMG; (d) converging DFS with modified QCPMG. The relative S/N ratios are given on the right. From R.S. Siegel, T.T. Nakashima, R.E. Wasylishen, Concepts Magn. Reson. Part A 26A (2005), 62. Reproduced by permission of Wiley Inc.

breadth of the CT, with a 'subspectrum' being acquired at each offset. The series of subspectra are then overlapped (skyline processed) or summed (co-addition processed) to produce the entire CT spectrum. In cases where the QCPMG method is used, the transmitter frequency offsets must be chosen so that the spikelets in different experiments overlap constructively. In our experience, the QCPMG sequence has been advantageous to achieve the needed S/N ratio for variable-offset experiments involving ^{35}Cl, due to its lower receptivity, while simple echoes are feasible for the bromine nuclides when they are present in ionic systems [51]. An example of the skyline processing method is presented in Fig. 6, where the QCPMG variable-offset approach has been applied to acquire the ^{35}Cl CT spectrum of indium trichloride tetrahydrate at 21.1 T. This method greatly expands the range of chlorine, bromine and iodine materials that can be studied with SSNMR, as experiments are not limited by the excitation bandwidth of the probe. In the future, the WURST-QCPMG method of O'Dell and Schurko, which allows for the efficient acquisition of broad spectra, will also be useful for the collection of the broad SSNMR spectra of $^{35/37}$Cl, $^{79/81}$Br, and ^{127}I [58,59].

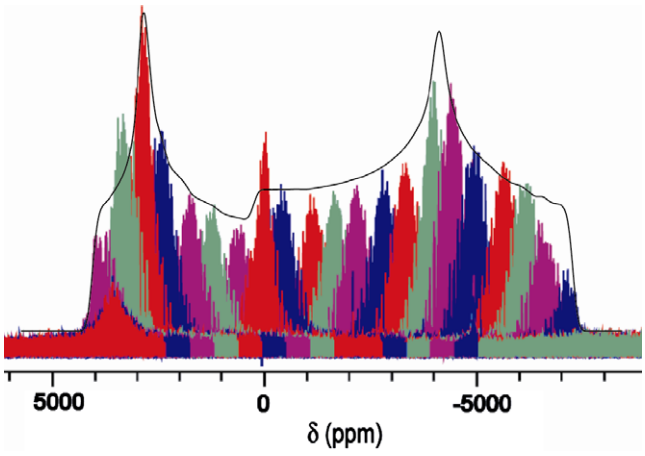

Fig. 6. Variable-offset chlorine-35 CT NMR spectrum of $InCl_3 \cdot 4H_2O$. The 25 QCPMG subspectra have been overlaid to give the shape of the overall spectrum, which covers about 1 MHz at 21.1 T. The solid line is an analytical simulation from which the following approximate parameters may be extracted: $C_Q(^{35}Cl) = 23.4$ MHz; $\eta_Q = 0.27$; $\delta_{iso} = 130$ ppm. Decreasing the offset used would reduce the oscillations in the envelope of the experimental pattern.

Other methods have been used in select chlorine, bromine, or iodine SSNMR studies. Satellite-transition spectroscopy (SATRAS), where the MAS NMR spectrum of the satellite transitions is collected and analyzed [60–62], was used by Trill et al. on a series of halide-containing sodalites [46]. More recently, Persons and Harbison collected ^{79}Br SSNMR spectra of several samples using their "slow turning reveals enormous anisotropic quadrupolar interactions" (STREAQI) method [63]. The STREAQI method was shown to characterize the quadrupolar parameters of sites with moderately large QIs (10–50 MHz) using very slow MAS rates (e.g., 300 Hz), although the current analysis method does not take into account CSA.

3.2. Extraction of SSNMR parameters

As mentioned above, the centreband of the CT under fast MAS conditions depends on δ_{iso}, C_Q, and η_Q and these parameters can typically be determined by line shape analysis (as implemented in WSolids [64,65], SIMPSON [66], or DMFIT [67], for example). Thus, where possible, the desired method to extract both the CS and QI tensor parameters for a sample is to first analyze the MAS spectrum to extract δ_{iso}, C_Q, and η_Q and then run a static experiment and perform a line shape analysis of that spectrum to extract the remaining parameters: Ω, κ, α, β, and γ. In cases where the QI is too great to obtain a MAS spectrum, the static spectrum must generally be fit with all eight parameters as variables. As there is often more than one combination of the eight parameters that can give

the same spectrum, collection of the spectrum at multiple fields is preferred, in order to confirm the accuracy of the determined parameters, as the same set of parameters must fit all the spectra acquired for a given material. Conveniently, in the case of chlorine and bromine there is a second "built-in" field, as there are two NMR-active isotopes, both in reasonable natural abundances, of those two elements. To a good approximation, the only parameter that changes when comparing the two isotopes of chlorine or bromine, is the C_Q value, due to each possessing a different Q value. In the case of chlorine, the chlorine-37 coupling constant is 78.8% that of the chlorine-37 value, while the bromine-81 coupling constant is 83.7% that of the value for bromine-79 [68]. In principle, one must be aware of possible isotope effects on the chemical shift, but these are expected to be negligible, particularly in the analysis of broad powder patterns.

4. Chlorine-35/37 experimental data

The types of materials that have been analyzed using $^{35/37}$Cl SSNMR include biological molecules, inorganic materials, and chlorine-containing glasses [7]. The chlorine chemical shift range is approximately 1100 ppm, ranging from −78.06 for CuCl [69] to 1049.3 ppm for $KClO_4$ [70] (both referenced to NaCl(*s*)) (Fig. 1).

Of the three quadrupolar halogens, the effects of CSA are most visible in chlorine NMR spectra as a result of the smaller Q value for both isotopes of chlorine. Thus, only for the chlorine nucleus have there been a significant number of samples for which the CS tensor has been characterized [7]. Chlorine CSA data are summarized in Table 3.

4.1. Simple chlorides

Selected SSNMR data for inorganic chloride salts are given in Tables 2 and 4. These tables, along with all other data tables in this review, are not intended to be comprehensive. They represent an overview of the available single crystal and powdered sample data, emphasizing studies we feel are significant to the field. In the case of the simple chlorides, this entails including those studies that provided accurate chemical shift data referenced to relatively common reference compounds. More comprehensive data tables and detailed discussion pertaining to several metal halides are available in our prior review [8].

Simple chloride salts have been popular materials of study by $^{35/37}$Cl SSNMR, due to the cubic environment about the chlorine nucleus in many such compounds. The high symmetry of these systems results in small $C_Q(^{35/37}Cl)$ values, which allows them to be analyzed in relatively low magnetic fields. The first chlorine SSNMR study appears to have been done by Kanda in 1955 on powdered samples of four simple salts: NaCl, CsCl, AgCl and TlCl [71]. The relative order of the chemical shifts was reported and rationalized by the suggestion that the shift increased with increasing bond covalency. In addition, the study demonstrates the ability to study these cubic materials at low magnetic fields (i.e., 0.300–0.622 T).

A comprehensive study of all the alkali metal chlorides was performed using powdered samples by Yamagata in 1964 and a chemical shift trend was noted [72]. This study found that, with the exception of lithium, the chlorine CS increased upon increasing the atomic number of the alkali metal. Yamagata concluded from this study that the dominant factor in determining the chlorine chemical shift was the orbital overlap between the halogen ion and its nearest and next nearest neighbours.

Additional comprehensive studies of cubic chloride salts were carried out several decades later. Weeding and Veeman studied NaCl, KCl, RbCl, CsCl and NH_4Cl [73]. The investigators collected MAS NMR spectra of powdered samples, and observed sharp lineshapes in which second-order quadrupolar broadening was absent. The absence of quadrupolar broadening demonstrated the absence of a QI, as expected due to the cubic arrangement of the ions in these salts. Both isotopes of chlorine were analyzed by the authors, and were found to have nearly identical chemical shifts, as would be expected in the absence of significant isotope effects. The chlorine chemical shift was found to correlate with the M–Cl bond distance, as well as the Sanderson electronegativity of the cation.

Shortly thereafter, Hayashi and Hayamizu [74] acquired both MAS and static chlorine NMR spectra for seven simple chloride salts: the alkali metal chlorides (LiCl, NaCl, KCl, RbCl, and CsCl), as well as CuCl and AgCl. The authors rationalized the chlorine chemical shifts in a similar manner to Yamagata, focusing on the orbital overlap between the nucleus and its neighbours [72]. In addition to the chlorine NMR spectra, the authors collected the ^{7}Li, ^{23}Na, ^{87}Rb, and ^{133}Cs MAS NMR spectra of the appropriate salts.

In 1992, Lefebvre reported ^{35}Cl chemical shifts for selected simple salts under static conditions [75]. The relationship between chemical shift and Sanderson electronegativity, noted previously [73], was confirmed. The possibility that earlier researchers were actually collecting the ^{35}Cl NMR spectrum for a hydrate of lithium chloride, $Li(H_2O)_x$, was proposed as an explanation for the anomalous chlorine chemical shift observed for 'LiCl'.

Honda examined several *n*-alkylammonium chlorides, n-$C_xH_{(2x+1)}NH_3Cl$ [76]. Some salts were deuterated, and it was found that in all cases, these salts had lower magnitudes of $C_Q(^{35}Cl)$, compared to their non-deuterated counterparts. It was also noted that the chlorine-35 C_Q followed an 'even-odd' trend in the highest temperature phase of the salts. The 'even' salts (x = 8 and 10) had much larger coupling constants compared to those of the 'odd' salts (x = 5, 7, 9). All $C_Q(^{35}Cl)$ magnitudes fell in the range of 1.0–1.5 MHz. Chlorine-35 NMR spectra of these salts and their deuterated counterparts are shown in Fig. 7.

There have been numerous additional studies on both single crystals and powdered samples of the simple chloride salts, and a variety of properties were measured [8]. Examples include using the temperature dependence of T_1 in NaCl and AgCl to calculate defect migration, the pressure and temperature dependence of $\delta_{iso}(^{35}Cl)$ in RbCl, and the effect of elastic strain on the chlorine CT line shape in NaCl, amongst others [39,77–81].

4.2. Chlorine in non-cubic inorganic and organometallic compounds

Chlorine quadrupolar parameters for non-cubic inorganic and organometallic compounds are presented in Table 4 and available CS tensor parameters are summarized in Table 3. Rossini et al. [52] very recently presented an extensive ^{35}Cl SSNMR study of a series of group IV transition metal organometallic complexes, including Cp_2TiCl_2, $CpTiCl_3$, Cp_2ZrCl_2, Cp_2HfCl_2, $Cp^*_2ZrCl_2$, $CpZrCl_3$, Cp^*ZrCl_3, $Cp_2ZrMeCl$, and $(Cp_2ZrCl)_2(\mu$-O) (Cp = cyclopentadienyl; Cp* = pentamethylcyclopentadienyl). Signal-enhancement techniques such as QCPMG, combined with variable-offset data acquisition and ultrahigh magnetic fields (21.1 T), were applied in this study. The values of $C_Q(^{35}Cl)$ were found to range from 12.8(5) MHz for one of the four chlorine sites in Cp^*ZrCl_3 to 22.1(5) MHz in Cp_2TiCl_2. Although this study is apparently the first to characterize chlorine in a "covalent" environment using powdered samples and modern high-field NMR methods, we note that the C_Q values are significantly lower than those known for covalently-bound chlorine atoms in organic molecules. For example, ^{35}Cl NQR data for a range of chlorine-containing organic heterocycles (e.g., 2-chloropyridine) indicate quadrupolar coupling constants on the order of 70 MHz [13]. An indirect NMR measurement of $C_Q(^{35}Cl)$ in 2-chloro-2-(phenylsulfonyl)-1-phenylpropanone, obtained by measuring the residual dipolar coupling in the ^{13}C CP/MAS NMR spectrum, yielded a value of −73 ± 2 MHz [82]. In this context, the values of

Table 3
Chlorine-35 chemical shift tensor data.[a]

Compound	δ_{iso}/ppm	δ_{11}/ppm	δ_{22}/ppm	δ_{33}/ppm	α,β,γ (deg)[b]	References
$CpTiCl_3$	500(150)[c]	925	400	175	80(30), 5(15), 5(30)	Rossini et al. [52]
Cp_2ZrCl_2	300(150)[c]	700	300	−100	2(10), 72(20), −70(20)	Rossini et al. [52]
Cp^*ZrCl_3 (sites 1 & 2)	400(200)[c]	617	467	117	10(90), 15(30), 0(90)	Rossini et al. [52]
Cp^*ZrCl_3 (sites 3 & 4)	200(200)[c]	Ω = 200(200)			–	Rossini et al. [52]
Butyldimethylimidazolium chloride	71.60(0.02)[d]	101.90	88.69	24.20	16(1), 82.5(0.5), −34(4)	Gordon et al. [90]
Butylmethylimidazolium chloride	71.65(0.05)[d]	96.66	65.13	53.16	78(2), 76(1), 12(2)	Gordon et al. [90]
Procaine HCl	96(6)[e]	166.8	79.3	41.8	95(15), 3(2), 32(8)	Hamaed et al. [88]
Tetracaine HCl	71(6)[e]	105.6	81.7	25.7	60(8), 8(5), 10(10)	Hamaed et al. [88]
Lidocaine HCl	100(4)[e]	170.6	68.8	60.6	12(3), 40(10), 80(3)	Hamaed et al. [88]
Lidocaine HCl polymorph 1,[f] site 1	85(10)[e]	97.7	79.7	77.7	90(40), 50(50), 60(40)	Hamaed et al. [88]
Lidocaine HCl polymorph 1,[f] site 2	110(10)[e]	126.5	122.0	81.5	5(5), 50(15), 40(40)	Hamaed et al. [88]
Bupivacaine HCl	96(10)[e]	142.7	102.7	42.7	105(20), 90(5), 5(5)	Hamaed et al. [88]
Bupivacaine HCl heated to 120 °C, site 1	118(10)[e]	174	166	14	10(10), 3(1), 0(2)	Hamaed et al. [88]
Bupivacaine HCl heated to 120 °C, site 2	95(10)[e]	180.3	84.3	20.3	18(4), 50(5), 80(5)	Hamaed et al. [88]
Bupivacaine HCl heated to 170 °C	118(5)[e]	162	150	42	10(10), 0(2), 50(50)	Hamaed et al. [88]
Alanine HCl	106(5)[e]	139	100	79	90(15), 0(15), 0(15)	Chapman and Bryce [50]
Aspartic acid HCl	102(5)[e]	150.8	79.5	75.8	0(20), 30(20), 93(20)	Chapman and Bryce [50]
Cysteine HCl monohydrate	104.2(0.5)[e]	135.9	106.8	69.9	155(20), 0(10), 0(20)	Chapman and Bryce [50]
Histidine HCl monohydrate	93(1)[e]	Ω < 150			–	Chapman and Bryce [50]
Methionine HCl	99(1)[e]	144	109	44	93(20), 163(15), 7(20)	Chapman and Bryce [50]
Threonine HCl	99(10)[e]	149.7	92.7	54.7	95(15), 0(10), 0(15)	Chapman and Bryce [50]
$MgCl_2 \cdot 6H_2O$	75.0(1.0)[e]	Ω < 75			–	Bryce and Bultz [83]
$CaCl_2 \cdot 2H_2O$	110.0(2.0)[e]	138.8	124.4	66.8	90(10), 82(5), 0(20)	Bryce and Bultz [83]
$SrCl_2$	188.2(1.0)[e]	188.2	188.2	188.2	–	Bryce and Bultz [83]
$SrCl_2 \cdot 2H_2O$	142.1(1.0)[e]	159.2	148.9	118.2	86(15), 75(5), 37(10)	Bryce and Bultz [83]
$SrCl_2 \cdot 6H_2O$	90.4(1.0)[e]	120.4	75.4	75.4	0(10), 90(10), 0(10)	Bryce and Bultz [83]
$BaCl_2 \cdot 2H_2O$ site 1	163.4(2.0)[e]	195.1	150.1	145.1	85(20), 32(10), 60(20)	Bryce and Bultz [83]
$BaCl_2 \cdot 2H_2O$ site 2	156.6(2.0)[e]	179.9	159.9	129.9	20(15), 8(10), 0(20)	Bryce and Bultz [83]
L-tryptophan HCl	105.0(1.0)[e]	139.8	107.4	67.8	90(15), 20(15), 2(20)	Bryce and Sward [48]
DL-arginine HCl monohydrate	91.5(1.0)[e]	117.7	96.7	60.2	85(15), 77.5(12.0), 30(30)	Bryce and Sward [48]
L-lysine HCl	105(2)[e]	119.7	101.5	93.7	0(20), 52(20), 0(20)	Bryce et al. [49]
L-serine HCl	120(30)[e]	Ω < 150			–	Bryce et al. [49]
L-glutamic acid HCl	102(1)[e]	135	102	69	9(20), 77(20), 6(20)	Bryce et al. [49]
L-proline HCl	37(5)[e]	74.2	25.7	11.2	48(20), 69(20), 9(20)	Bryce et al. [49]
L-isoleucine HCl	96(20)[e]	Ω = 75(30); κ < 0.85			20(20), 12(20), 0(20)	Bryce et al. [49]
L-valine HCl	90(10)[e]	145.2	104.6	20.2	65(20), 0(20), 0(20)	Bryce et al. [49]
L-phenylalanine HCl	96(5)[e]	154.9	107.2	25.9	91(20), 13(20), 10(20)	Bryce et al. [49]
Glycine HCl	101(5)[e]	146	111	46	95(20), 0(20), 0(20)	Bryce et al. [49]
L-cysteine ethyl ester HCl	53.2(0.5)[c]	83.0	40.7	36.0	β = 90	Bryce et al. [53]
L-tyrosine HCl	49.3(0.5)[c]	Ω < 150			–	Bryce et al. [53]
L-cysteine methyl ester HCl	48.2(0.7)[c]	Ω = 45(15)			–	Bryce et al. [53]
Quinuclidine HCl	9.7(10.0)[c]	Ω = 50(20)			–	Bryce et al. [53]
Tris sarcosine $CaCl_2$	14.7(10.0)[c]	Ω < 150			–	Bryce et al. [53]
$LiAl_2(OH)_6ClO_4 \cdot nH_2O$	Spectra obtained at several relative humidities	Ω ranges from ~10 to ~160				Hou et al. [131,132]; Hou and Kirkpatrick[133]
$Mg_3Al(OH)_6ClO_4 \cdot nH_2O$						
$LiAl_2(OH)_6Cl \cdot nH_2O$						
NH_4ClO_4	917.5(0.7)[c]	932.8	918.9	900.8	–	Bastow and Stuart [97]
p-dichlorobenzene	666.7[g]	3000(1000)	0(1000)	−1000(1000)	0,0,0 (assumed)	Creel et al. [134]
$NaClO_3$	–	Ω = 40(7)				Kawamori and Itoh [135]

[a] Errors are given in parentheses; all parameter definitions are provided in the main text.
[b] Euler angles describing the relationship between the PAS of the CS tensor and that of the EFG tensor.
[c] With respect to infinitely dilute NaCl(*aq*).
[d] With respect to 0.1 M NaCl in D_2O.
[e] With respect to NaCl(*s*).
[f] See Ref. [88] for details on sample preparation.
[g] No chemical shift reference given.

$C_Q(^{35}Cl)$ obtained for the group IV transition metal complexes suggest that the chlorine bonding environment contains more ionic character than in the organic systems. Values of $C_Q(^{35}Cl)$ for chlorines in ionic environments within inorganic and organic systems (where Cl^- is a counterion) can approach 10 MHz (e.g., the $C_Q(^{35}Cl)$ value for aspartic acid hydrochloride is 7.1 ± 0.1 MHz [50]).

Rossini et al. also provided valuable chlorine chemical shift tensor information for the group IV transition metal chloride complexes [52]. Perhaps most interesting are the isotropic chemical shifts, which fall in between the previously known ranges for chloride ions (approximately −100 to +200 ppm, with respect to NaCl(*s*)) and perchlorate ions (approximately 900–1100 ppm). For instance, the value for $CpTiCl_3$ is 545 ± 150 ppm with respect to the same reference. The measured spans of the chlorine CS tensors are quite large relative to other literature values; for example, a value of 800 ± 500 ppm was reported for Cp_2ZrCl_2. This is consistent with a more covalent bonding environment, relative to the known ionic systems.

In the same study, the authors combined ^{35}Cl SSNMR results with X-ray diffraction data and quantum chemical calculations to demonstrate that Cp_2ZrHCl (Schwartz's reagent) exists as a dimer in the solid state [52]. They also attempted to establish definitive

Table 4
Selected chlorine-35 quadrupolar parameters and isotropic chemical shifts for inorganic and organometallic chlorides.[a]

Compound	δ_{iso}/ppm	$C_Q(^{35}Cl)$/MHz	η_Q	References
Cp_2TiCl_2[b]	500(500)[c]	22.1(0.5)	0.61(0.03)	Rossini et al. [52]
Cp_2ZrCl_2	300(150)[c]	16.0(0.5)	0.72(0.04)	Rossini et al. [52]
Cp_2HfCl_2	400(500)[c]	17.1(0.4)	0.65(0.05)	Rossini et al. [52]
$Cp^*_2ZrCl_2$[d]	400(400)[c]	16.7(0.4)	0.73(0.03)	Rossini et al. [52]
$CpTiCl_3$	500(150)[c]	15.5(0.4)	0.54(0.05)	Rossini et al. [52]
$Cp_2ZrMeCl$	400(400)[c]	13.7(0.4)	0.75(0.10)	Rossini et al. [52]
$(Cp_2ZrCl)_2(\mu$–O)	300(400)[c]	16.3(0.4)	0.43(0.07)	Rossini et al. [52]
Cp^*ZrCl_3 (four sites)	400(200)[c]	12.8(0.5)	0.10(0.10)	Rossini et al. [52]
	400(200)[c]	13.3(0.5)	0.12(0.10)	
	200(200)[c]	14.6(0.5)	0.88(0.10)	
	200(200)[c]	14.0(0.5)	0.80(0.10)	
$CpZrCl_3$ (multiple sites)	300[c]	14.8–18.6	0.7–0.8	Rossini et al. [52]
Cp_2ZrHCl	80(50)[c]	19.7(0.3)	0.20(0.04)	Rossini et al. [52]
$CaCl_2 \cdot 2H_2O$	110.0(2.0)[e]	4.26(0.03)	0.75(0.03)	Bryce et al. [83]
$BaCl_2$	site 1: 124(5)[f]	site 1: 3.5(0.1)	0.15(0.05)	Stebbins and Du [84]
	site 2: 219(5)[f]	site 2: 3.95	0.1	
$BaCl_2 \cdot 2H_2O$	site 1: 163.4(2.0)[e]	site 1: 2.19(0.08)	0	Bryce and Bultz [83]
	site 2: 156.6(2.0)[e]	site 2: 3.42(0.08)	0.31(0.10)	
VCl_2	–	~4(2 sites)	0(assumed)	Tabak et al. [136]
$MgCl_2 \cdot 6H_2O$	75.0(1.0)[e]	3.02(0.05)	0	Bryce and Bultz [83]
$SrCl_2$	140.8[f]	–	–	Lefebvre [75]
$SrCl_2$	188.2(1.0)[e]	~0	–	Bryce and Bultz [83]
$SrCl_2 \cdot 2H_2O$	142.1(1.0)[e]	1.41(0.02)	0.80(0.10)	Bryce and Bultz [83]
$SrCl_2 \cdot 6H_2O$	90.4(1.0)[e]	3.91(0.05)	0	Bryce and Bultz [83]
$Mn(CO)_5Cl$	–	36.07(0.01) (303 K)	0.050(0.005)	Spiess and Sheline [137]
$FeCl_2$	–	4.74(0.01)	–	Barnes and Segel [138]
	–	4.74(0.02)	–	Jones and Segel [139]
$K_2CuCl_4 \cdot 2H_2O$	–	(4.2 K)	(4.2 K)	Choh and Stager [140]
		site 1: 18.98	0.1883	
		site 2: 3.490	0.877	
		(77 K)	(77 K)	
		site 1: 19.07	0.1902	
		site 2: 3.434	0.895	
		(295 K)	(295 K)	
		site 1: 19.05	0.183	
		site 2: 3.262	0.945	
		(340 K)	(340 K)	
		site 2: 3.229	0.97	
BaFCl	–	2.38	0	Bastow et al. [141]
Ag_5Te_2Cl				
α-form	−12.9(0.5)[f] (356 K)	–	–	Brinkmann et al. [142]
β-form	−8.9[f] (296 K)		–	
γ-form	−4.8(0.5)[f] (216 K)		–	

[a] Errors are given in parentheses; all parameter definitions are provided in the main text.
[b] Cp = cyclopentadienyl.
[c] With respect to infinitely dilute NaCl(*aq*).
[d] Cp^* = pentamethylcyclopentadienyl.
[e] With respect to NaCl(*s*).
[f] With respect to 1 M NaCl(*aq*).

^{35}Cl NMR fingerprints for terminal vs. bridging chloride ligands in the systems studied. In the case of Cp^*ZrCl_3, the bridging chlorine atoms gave rise to a much larger CT powder pattern (Fig. 8), while in the case of $CpZrCl_3$, one type of bridging chlorine gave rise to a *narrower* powder pattern than did the terminal chlorines. While further studies will be required to determine if a general relationship exists between the chlorine QI and the nature of the chlorine site, these authors were able to demonstrate, importantly, that the two different types of sites were resolvable by ^{35}Cl SSNMR in their systems [52].

Selected chlorine quadrupolar coupling data for solid alkaline earth metal chlorides are presented in Table 4. The chlorine CS tensors have also been characterized and these data appear in Table 3. Peaks initially assigned to isotropic ^{35}Cl chemical shifts [75] were later found to correspond to discontinuities from second-order quadrupolar powder patterns, which were present due to a non-zero QI at the chlorine nucleus [83]. The chemical shift originally reported for $SrCl_2$, 140.8 ppm (referenced to 1 M NaCl(*aq*)), was found to be correct, as a result of the tetrahedral environment at the chlorine and the resulting absence of second-order broadening due to a QI. Bryce and Bultz reported a $^{35/37}$Cl SSNMR study of several alkaline earth chlorides and their hydrates [83]. Six materials were analyzed at 11.75 and 21.1 T under static and MAS conditions, allowing for the determination of both the EFG and CS tensor parameters. An example is given in Fig. 9; the fits at multiple fields for both nuclei demonstrate the reliability of the extracted spectral parameters. Chlorine-35 C_Q values were found to range from ~0 MHz ($SrCl_2$) to 4.26 ± 0.03 MHz ($CaCl_2 \cdot 2H_2O$), while chlorine chemical shifts ranged from 75.0 ± 1.0 ppm ($MgCl_2 \cdot 6H_2O$) to 188.2 ± 1.0 ppm ($SrCl_2$), referenced to NaCl(*s*). In addition to fully characterizing the chlorine EFG and CS tensors for the materials studied, the sensitivity of chlorine SSNMR to pseudo-polymorphism was demonstrated by the significant differences in the chlorine NMR parameters of $SrCl_2$ ($C_Q(^{35}Cl) \sim 0$ MHz) and its hydrates, $SrCl_2 \cdot 2H_2O$ ($C_Q(^{35}Cl) = 1.41 \pm 0.02$) and $SrCl_2 \cdot 6H_2O$ ($C_Q(^{35}Cl) = 3.91 \pm 0.05$). In addition, the ability to monitor the conversion between these different pseudo-polymorphs by ^{35}Cl SSNMR has been noted [8,83].

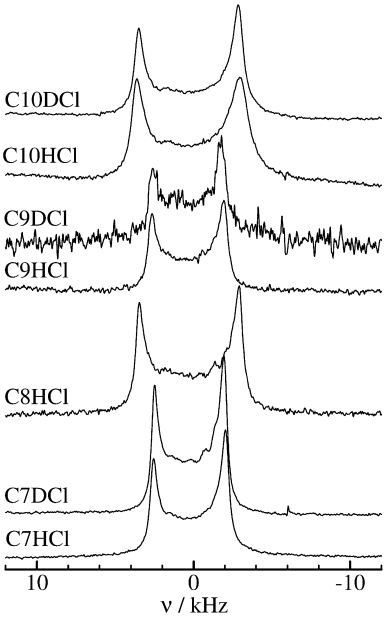

Fig. 7. Chlorine-35 CT NMR spectra of *n*-$C_xH_{(2x+1)}NH_3$–Cl (CxHCl) and *n*-$C_xH_{(2x+1)}ND_3Cl$ (CxDCl) collected under stationary conditions in a magnetic field of 7.04 T. From H. Honda, Z. Naturforsch 58a (2003), 623. Reproduced by permission of the Verlag der Zeitschrift für Naturforschung.

Stebbins and co-workers collected ^{35}Cl NMR spectra of solid powdered $BaCl_2$ and $CaCl_2$ during their studies of chlorine-containing glasses [84,85]. In both instances, the chlorine-35 C_Q value and the chlorine chemical shift are of similar magnitude, but clearly distinct from, those observed for the hydrated salts studied by Bryce and Bultz [83]. This is another demonstration of the sensitivity of the ^{35}Cl NMR spectrum to the hydration state of the material studied. In approximate terms, the more strongly hydrated pseudopolymorphs tend to have smaller chemical shifts.

4.3. Organic chlorides and hydrochlorides

Selected chlorine quadrupolar parameters for hydrochloride salts appear in Table 5. Organic hydrochloride salts have been popular materials of study in the last decade, and rigorous spectral analyses have been carried out, providing both the EFG and CS tensor parameters, as demonstrated by the prevalence of these materials in Tables 3 and 5.

The first hydrochloride to be analyzed by chlorine SSNMR appears to be a powdered sample of cocaine hydrochloride [86]. The ^{35}Cl NMR spectrum was collected at 7.0 T using a Hahn-echo experiment and variable-offset data acquisition. The measured $C_Q(^{35}Cl)$ value is 5.027 MHz. Bryce et al. later studied a series of organic hydrochlorides, and demonstrated the utility of chlorine-35/37 SSNMR in the study of chlorine atoms within hydrogen bonding environments [53]. Spectra for L-tyrosine HCl, L-cysteine methyl ester HCl, L-cysteine ethyl ester HCl and quinuclidine HCl were collected at 18.8 and 9.4 T, using a variety of techniques. These included Hahn-echoes under MAS and static conditions, as well as the QCPMG sequence under stationary conditions. The EFG tensor parameters were reported for all four salts, while the CS tensor parameters were given for L-cysteine ethyl ester HCl.

Studies of additional amino acid hydrochlorides were reported in subsequent publications. In 2005, Gervais et al. studied four amino acid hydrochlorides using multinuclear magnetic resonance experiments, including some performed on ^{35}Cl [87]. The authors provided the isotropic CS and EFG tensor parameters for glycine HCl, L-valine HCl and L-glutamic acid HCl and confirmed the reported parameters for L-tyrosine HCl. First principles calculations predicted relatively small chlorine CS tensor spans ranging from 78 to 157 ppm [87]. Bryce and co-workers examined the majority of the amino acid hydrochlorides in three reports published in 2006 and 2007, using these compounds as simple models for chloride ion binding sites in ion channels [48–50] (see Figs. 10 and 11). The experiments were carried out at fields of 11.75 and 21.1 T, under stationary and, when possible, MAS conditions. In addition to the EFG tensor parameters, the CS tensor parameters for the majority of these salts were determined. The extraction of CSA information benefited greatly from the ultrahigh-field experiments, as the broadening due to the QI decreases with increased field while the effects of the CSA increase. It was found that both the quadrupolar and CS tensor parameters were highly dependent on the specific local and electronic environment, as a wide range of parameters were measured, despite some similarities in the chlorine environments between different amino acid hydrochlorides. The value of $C_Q(^{35}Cl)$ was found to generally decrease as the number of hydro-

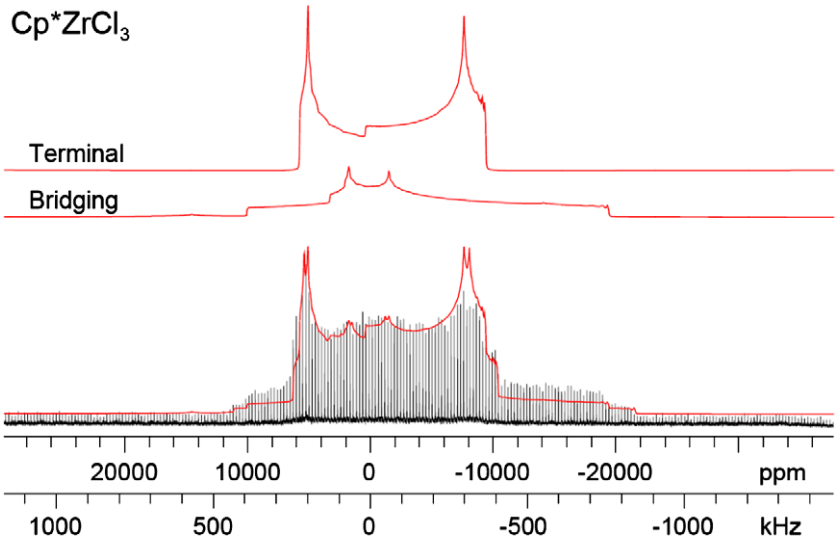

Fig. 8. Solid-state ^{35}Cl QCPMG NMR spectra and simulations for Cp^*ZrCl_3. The final simulation represents four sites (two bridging and two terminal); representative simulations of bridging and terminal sites are shown above (B_0 = 9.4 T). From Rossini et al. J. Am. Chem. Soc. 131 (2009), 3317. Reproduced by permission of the American Chemical Society.

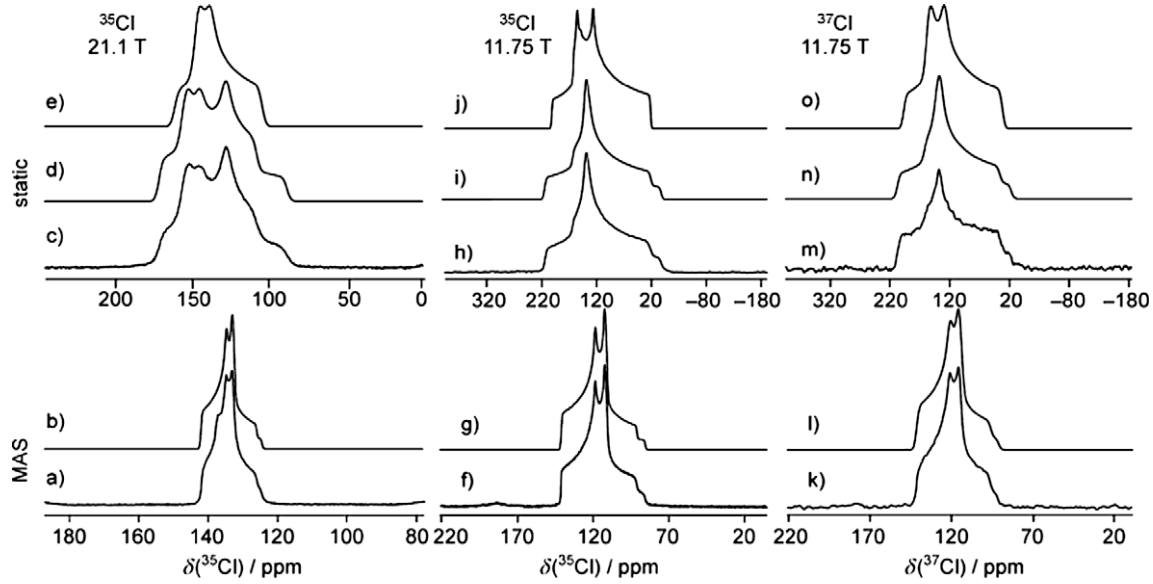

Fig. 9. $^{35/37}$Cl NMR spectra of solid powdered $SrCl_2.2H_2O$. (a), (f) ^{35}Cl spectra of a MAS sample obtained at 21.1 and 11.75 T, respectively. (b) and (g) show best-fit simulated spectra. (k) ^{37}Cl spectrum of a MAS sample obtained at 11.75 T. (l) The best-fit simulated spectrum. (c), (h) ^{35}Cl spectra of a stationary sample obtained at 21.1 and 11.75 T, respectively. The corresponding best-fit simulated spectra are shown in (d) and (i). The span of the CS tensor is set to zero in (e) and (j) to demonstrate the large effect that the anisotropy of the CS tensor has on the spectrum. (m) ^{37}Cl spectrum of a stationary powdered sample obtained at 11.75 T. The best-fit simulated spectrum is shown in (n), and a simulated spectrum for which the CS tensor span is set to zero is shown in (o). From Bryce and Bultz, Chem. Eur. J. 13 (2007), 4786. Copyright Wiley-VCH Verlag GmbH & Co. KGaA. Reproduced with permission.

gen bonds around chlorine increased; however, the symmetry around the chlorine was also an important consideration. The information available from the quadrupolar parameters and CS tensors is complementary, as there was no general correlation found between the two sets of data; for example, a larger value of C_Q does not necessarily correspond to a larger CS span. The chlorine-35 C_Q magnitudes range from 7.1 ± 0.1 MHz (aspartic acid HCl) to 2.03 ± 0.02 MHz (DL-arginine HCl monohydrate) [48–50]. The chlorine chemical shifts for these salts were found to be 90 to 106 ppm (referenced to NaCl(*s*)), with only proline HCl and serine HCl lying outside this range [48–50]. Quantum chemical calculations of the EFG and CS tensors were validated on the set of experimental data for the amino acid hydrochlorides, and then applied to estimate the chlorine C_Q for the ClC chloride ion channel (Fig. 12). The value obtained, $C_Q(^{35}Cl) = -2.07$ MHz, indicates that future ^{35}Cl SSNMR studies on chloride ion channels, or more sophisticated models for these channels, will not be hampered by broad CT resonances.

Hamaed et al. [88] used ^{35}Cl SSNMR to study the biologically important hydrochloride salts of four local anesthetic pharmaceuticals: procaine HCl, tetracaine HCl, monohydrated lidocaine HCl (LH), and monohydrated bupivacaine HCl (BH). Complete EFG and CS tensor parameters were provided for all materials studied, and again the sensitivity of the parameters to slight changes in structure, was observed. The chlorine-35 C_Q values observed in this study range from 2.52 to 6.00 MHz while the chlorine chemical shifts range from 71 to 118 ppm (referenced to NaCl(*s*)), which is similar to other organic hydrochlorides [48–50,87]. Quantum chemical calculations were performed in order to further the relationship between the chlorine NMR parameters and the number of short hydrogen bonds around the chloride ion [88]. The authors demonstrated that the sensitivity of ^{35}Cl SSNMR is great enough to easily distinguish between polymorphs of the same material (polymorphic structures of both LH and BH). Chlorine-35 NMR spectra were shown to be superior to ^{13}C NMR and powder X-ray diffraction methods for distinguishing between polymorphs in certain cases, most notably for a pair of high-temperature polymorphs of BH. The ^{35}Cl NMR spectra of three BH polymorphs are shown in Fig. 13. In the context of the results of Hamaed et al., one possible application of high-field ^{35}Cl SSNMR could be the identification of polymorphs or solvates in a pharmaceutical sample. The success of the approach will be limited by the (*a priori* unknown) size of the QI in a hypothetical impurity component (e.g., another polymorph, etc.), since a large QI would lead to a very broad CT signal, which would be buried in the baseline for very low concentrations, while an impurity with a very small QI would be easily detected at low concentrations due to the narrow line width of the CT in such a sample.

Frydman and co-workers have introduced a two-dimensional 'relaxation-assisted' spectroscopic method (RAS) to resolve multiple powder patterns arising from half-integer spin quadrupolar nuclei under stationary conditions [89]. Shown in Fig. 14 is an application of the method to resolve the ^{35}Cl resonances in a mixture of two hydrochloride salts. This method could prove to be useful in resolving multiple magnetically non-equivalent sites in a given sample; however, it relies on a significant difference in relaxation times to achieve resolution.

Gordon, Brouwer, and Ripmeester have reported a ^{35}Cl SSNMR study of several chlorine-containing ionic liquids at 9.4 and 21.1 T [90]. The four samples studied are solids at room temperature: methyl-*N*-butylpyridinium chloride ([MBPyri]Cl), butyldimethylimidazolium chloride ([BMMIM]Cl), ethylmethylimidazolium chloride ([EMIM]Cl), and butylmethylimidazolium chloride ([BMIM]Cl). Values of $C_Q(^{35}Cl)$ were found to be quite small, ranging from 0.805 ± 0.005 MHz for site 2 of [EMIM]Cl to 1.500 ± 0.002 MHz for [BMIM]Cl. Chemical shift tensor spans were extracted in two cases: 77.7 ± 0.2 ppm for [BMMIM]Cl and 43.5 ± 0.5 ppm for [BMIM]Cl and are consistent with the spans observed for other organic hydrochlorides (Table 3). The ^{35}Cl MAS NMR spectrum of [EMIM]Cl obtained at 21.1 T is impressive in that all four crystallographic sites are resolved (Fig. 15). The small values of $C_Q(^{35}Cl)$ suggest that $^{79/81}$Br and ^{127}I SSNMR of the bromide and iodide analogues of these ionic liquids should be feasible, assuming that the structures are isomorphic. Indeed, Gordon

Table 5
Selected chlorine-35 quadrupolar parameters and isotropic chemical shifts for organic chlorides and hydrochlorides.[a]

Compound	δ_{iso}/ppm	$C_Q(^{35}Cl)$/MHz	η_Q	References
Butyldimethylimidazolium chloride	71.60(0.02)[b]	0.978(0.004)	0.10(0.02)	Gordon et al. [90]
Butylmethylimidazolium chloride	71.65(0.05)[b]	1.500(0.002)	0.390(0.005)	Gordon et al. [90]
Ethylmethylimidazolium chloride	site 1: 91.72(0.03)[b]	0.808(0.004)	0.95(0.01)	Gordon et al. [90]
	site 2: 74.98(0.04)[b]	0.805(0.005)	0.20(0.02)	
	site 3: 71.36(0.04)[b]	0.884(0.004)	0.86(0.01)	
	site 4: 60.60(0.03)[b]	0.972(0.005)	0.80(0.01)	
Butylmethylpyridinium chloride	site 1: 83.15(0.07)[b]	0.857(0.008)	0.525(0.005)	Gordon et al. [90]
	site 2: 70.56(0.04)[b]	0.889(0.008)	0.08(0.08)	
Tyrosine HCl	94.7(0.5)[c]	2.23(0.02)	0.72(0.03)	Bryce et al. [53]
	95(1)[c]	2.3(0.1)	0.7(0.1)	Gervais et al. [87]
Glycine HCl	117(1)[c]	6.5(0.1)	0.6(0.1)	Gervais et al. [87]
	101(5)[c]	6.42(0.05)	0.61(0.03)	Bryce et al. [49]
L-valine HCl	114(1)[c]	6.0(0.1)	0.5(0.1)	Gervais et al. [87]
	90(10)[c]	5.89(0.05)	0.51(0.05)	Bryce et al. [49]
L-glutamic acid HCl	104(1)[c]	3.7(0.1)	0.6(0.1)	Gervais et al. [87]
	102(1)[c]	3.61(0.01)	0.65(0.02)	Bryce et al. [49]
Quinuclidine HCl	9.7(10.0)[d]	5.25(0.02)	0.05(0.01)	Bryce et al. [53]
L-cysteine ethyl ester HCl	53.2(0.5)[d]	3.78(0.02)	0.03(0.03)	Bryce et al. [53]
L-cysteine methyl ester HCl	48.2(0.7)[d]	2.37(0.01)	0.81(0.03)	Bryce et al. [53]
Cysteine HCl monohydrate	104.2(0.5)[c]	3.92(0.01)	0.47(0.02)	Chapman and Bryce [50]
Cocaine HCl	~0[c]	5.027	0.2(0.05)	Yesinowski et al. [86]
L-lysine HCl	105(2)[c]	2.49(0.01)	0.42(0.02)	Bryce et al. [49]
L-serine HCl	120(30)[c]	3.0 (0.3)	0.8(0.2)	Bryce et al. [49]
L-proline HCl	37(5)[c]	4.50(0.05)	0.63(0.05)	Bryce et al. [49]
L-isoleucine HCl	96(20)[c]	4.39(0.05)	0.25(0.03)	Bryce et al. [49]
L-phenylalanine HCl	96(5)[c]	6.08(0.05)	0.52(0.03)	Bryce et al. [49]
L-tryptophan HCl	105.0(1.0)[c]	5.05(0.04)	0.86(0.03)	Bryce and Sward [48]
DL-arginine HCl monohydrate	91.5(1.0)[c]	2.035(0.020)	0.98(0.02)	Bryce and Sward [48]
Alanine HCl	106(5)[c]	6.4(0.1)	0.75(0.06)	Chapman and Bryce [50]
Aspartic acid HCl	102(5)[c]	7.1(0.1)	0.42(0.05)	Chapman and Bryce [50]
Histidine HCl monohydrate	93(1)[a]	4.59(0.03)	0.46(0.02)	Chapman and Bryce [50]
Methionine HCl	99(1)[c]	4.41(0.02)	0.35(0.03)	Chapman and Bryce [50]
Threonine HCl	99(10)[c]	5.4(0.1)	0.94(0.02)	Chapman and Bryce [50]
Procaine HCl	96(6)[c]	4.87(0.07)	0.28(0.04)	Hamaed et al. [88]
Tetracaine HCl	71(6)[c]	6.00(0.10)	0.27(0.04)	Hamaed et al. [88]
Lidocaine HCl	100(4)[c]	4.67(0.07)	0.77(0.03)	Hamaed et al. [88]
Lidocaine HCl, polymorph 1	site 1: 85(10)[c]	site 1: 2.52(0.12)	0.95(0.05)	Hamaed et al. [88]
	site 2: 110(10)[c]	site 2: 5.32(0.10)	0.32(0.10)	
Bupivacaine HCl	96(10)[c]	3.66(0.10)	0.72(0.08)	Hamaed et al. [88]
Bupivacaine HCl heated to 120 °C	site 1: 118(10)[c]	site 1: 4.75(0.20)	0.65(0.10)	Hamaed et al. [88]
	site 2: 95(10)[c]	site 2: 5.85(0.20)	0.26(0.04)	
Bupivacaine HCl heated to 170 °C	118(5)[c]	4.58(0.05)	0.56(0.06)	Hamaed et al. [88]
n-$C_5H_{11}NH_3Cl$	–	1.143(0.001) (315 K)	–	Honda [76]
n-$C_7H_{15}NH_3Cl$	–	1.401(0.001) (300 K)	–	Honda [76]
n-$C_8H_{17}NH_3Cl$	–	1.501(0.001) (315 K)	–	Honda [76]
n-$C_9H_{19}NH_3Cl$	–	1.303(0.002) (320 K)	–	Honda [76]
n-$C_{10}H_{21}NH_3Cl$	–	1.469(0.001) (325 K)	–	Honda [76]
n-$C_7H_{15}ND_3Cl$	–	1.375(0.001) (300 K)	–	Honda [76]
n-$C_9H_{19}ND_3Cl$	–	1.280(0.002) (320 K)	–	Honda [76]
n-$C_{10}H_{21}ND_3Cl$	–	1.452(0.002) (325 K)	–	Honda [76]
Tris sarcosine $CaCl_2$	14.7(10.0)[d]	4.04(0.03)	0.62(0.02)	Bryce et al. [53]
$C_4H_9NH_3Cl$; $C_4H_9ND_3Cl$	–	~1.2–0.85 on heating from 300–480 K	~0	Hattori et al. [143]

[a] Errors are given in parentheses.
[b] With respect to 0.1 M NaCl in D_2O.
[c] With respect to NaCl(s).
[d] With respect to infinitely dilute NaCl(aq).

et al. have reported very promising preliminary data in this regard [91]. One of the important conclusions from the chlorine work noted above is that the SSNMR parameters are comparable to the values known for other organic hydrochlorides, which do not exhibit ionic liquid properties. Further work on these compounds could have an impact on the controversy in the literature over whether ionic liquids exhibit some unique "structure" in the liquid state [90,92–94].

4.4. Perchlorates

The experimental data for perchlorates (ClO_4^-) are summarized in Table 6. The chlorine site symmetry is approximately T_d in all the perchlorates studied, but the small deviation from tetrahedral symmetry results in a nonzero QI at the chlorine nuclei in these salts. The chlorine C_Q values are relatively small however, and they have been popular materials to study by chlorine SSNMR [70,95–103].

The first chlorine SSNMR spectrum of a perchlorate appears to have been published by Jurga et al. in their study of some multimethylammonium perchlorates in 1986 [95]. The ^{35}Cl C_Qs in these materials were found to be relatively small, as expected, with the largest being 1.120 MHz for phase III of dimethylammonium perchlorate. In 1991 and 1992, Tarasov et al. released two publications which report on three alkali metal perchlorates [98,99]. Chlorine-35 SSNMR spectra were collected at 7.04 T under stationary condi-

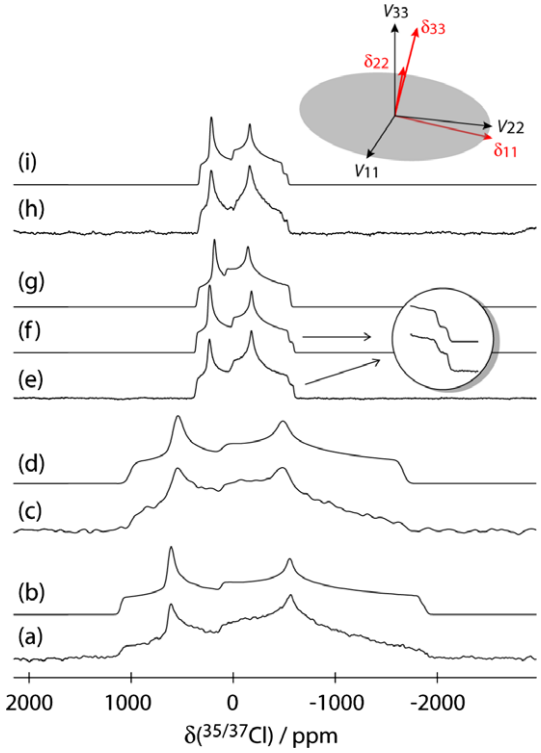

Fig. 10. Chlorine-35/37 SSNMR spectra of L-phenylalanine HCl under stationary conditions. Simulated spectra are shown above the experimental spectra. (a) ^{35}Cl at 11.75 T; (c) ^{37}Cl at 11.75 T; (e) ^{35}Cl at 21.1 T; (h) ^{37}Cl at 21.1 T. The relative orientation of the EFG and CS PASs are shown at the top. From Bryce et al. J. Am. Chem. Soc. 128 (2006), 2121. Reproduced by permission of the American Chemical Society.

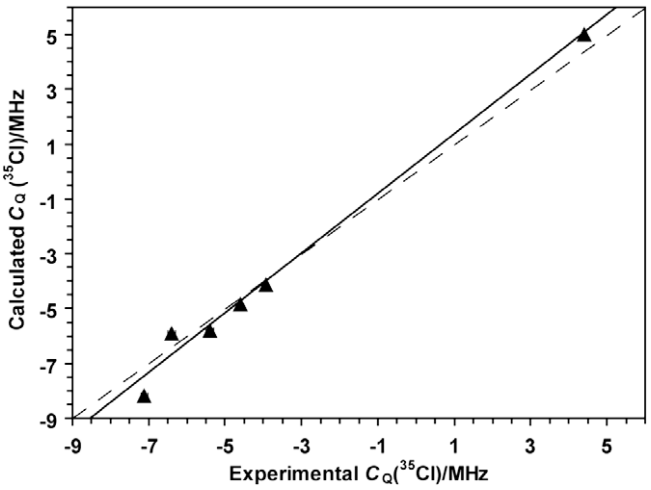

Fig. 11. Comparison between experimentally determined C_Q(^{35}Cl) for a series of amino acid hydrochlorides, on the *x*-axis, and the calculated values, on the *y*-axis. The equation for the line of best fit (solid line) is $y = 1.0892x + 0.2055$; $R = 0.994$. The line $y = x$ is represented by the dashed line. From R.P. Chapman and D.L. Bryce, Phys. Chem. Chem. Phys. 9 (2007), 6219. Further details on the calculations are given in reference [50]. Reproduced by permission of the PCCP Owner Societies.

tions. C_Q(^{35}Cl) values of ~0.63, 0.60, and 0.51 MHz were determined for $CsClO_4$, $RbClO_4$, and $KClO_4$ respectively; however, the effects of CSA were not considered.

A notable study of several perchlorates by Skibsted and Jakobsen was published in 1999 [70]. In this report, powdered samples

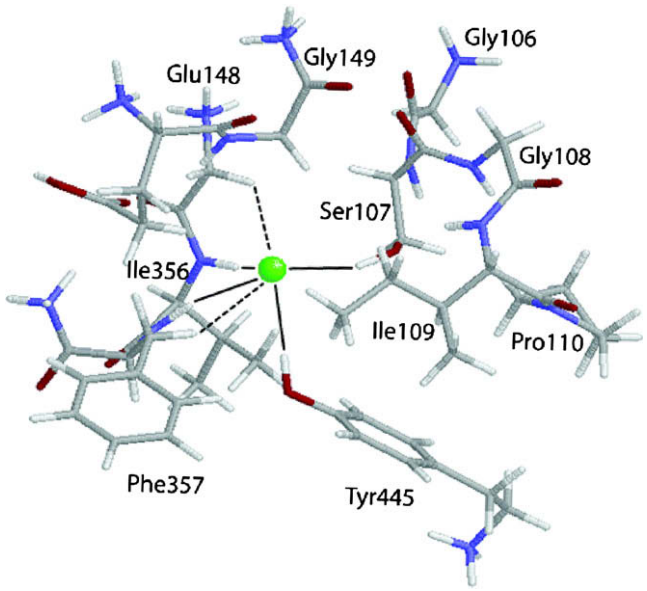

Fig. 12. Model of the chloride ion binding site in the ClC transport channel (PDB entry 1KPL) [3]. From Bryce et al. J. Am. Chem. Soc. 128 (2006), 2121. Reproduced by permission of the American Chemical Society.

of thirteen different perchlorates were analyzed using static, MAS and SATRAS methods. Both the ^{35}Cl and ^{37}Cl isotopes were studied. Typical CT and ST spectra for $LiClO_4$ are shown in Fig. 16. The sensitivity of the observed chlorine NMR spectrum to the hydration state of the sample was also demonstrated (anhydrous $LiClO_4$ compared with its trihydrate). Simulation of the chlorine MAS NMR spectra allowed for the determination of precise values of the chlorine chemical shift, C_Q, and η_Q values for all 13 salts. Included in this study were the perchlorates examined previously by Tarasov et al., and the C_Q(^{35}Cl) values determined in this study differ slightly, with values of 0.585, 0.537, and 0.441 MHz, for $CsClO_4$, $RbClO_4$, and $KClO_4$, respectively [98,99,70]. The chemical shifts observed for the perchlorates range from 1029.6–1049.3 ppm (referenced to NaCl(*s*)); these are much greater than those observed for chlorides, due to increased paramagnetic contributions to the shielding tensor.

4.5. Glasses and sodalites

Experimental data for glasses, sodalites, and all other chlorine-containing materials are summarized in Table 7. As mentioned above, Stebbins and co-workers have carried out multiple studies of chlorine-containing silicate and aluminosilicate glasses using MAS NMR at 14.1 and 18.8 T [84,85]. The chlorine-35 C_Q values vary between 3.0 and 4.4 MHz in different silicate glasses and from 2.9 to 3.6 MHz in aluminosilicate glasses. The authors proposed a correlation between the chlorine chemical shift and the M–Cl bond distance.

Trill et al. have published multiple studies on halogen-containing sodalites, the most extensive having been published in 2003 [46]. In this study, powdered samples of chloride-containing mixed halide sodalites were analyzed using ^{35}Cl MAS and SATRAS NMR. The authors reported the chlorine chemical shifts and chlorine-35 quadrupolar products ($P_Q = C_Q(1 + \eta_Q/3)^{1/2}$) for many different compositions of these sodalites, finding that P_Q was very small and constant at 0.2 ± 0.1 MHz, regardless of the percentage of Cl^- in the cages. The authors also reported the first application of MQMAS to a chlorine-containing system, using the pulse sequence to distinguish between two different chlorine sites with chlorine

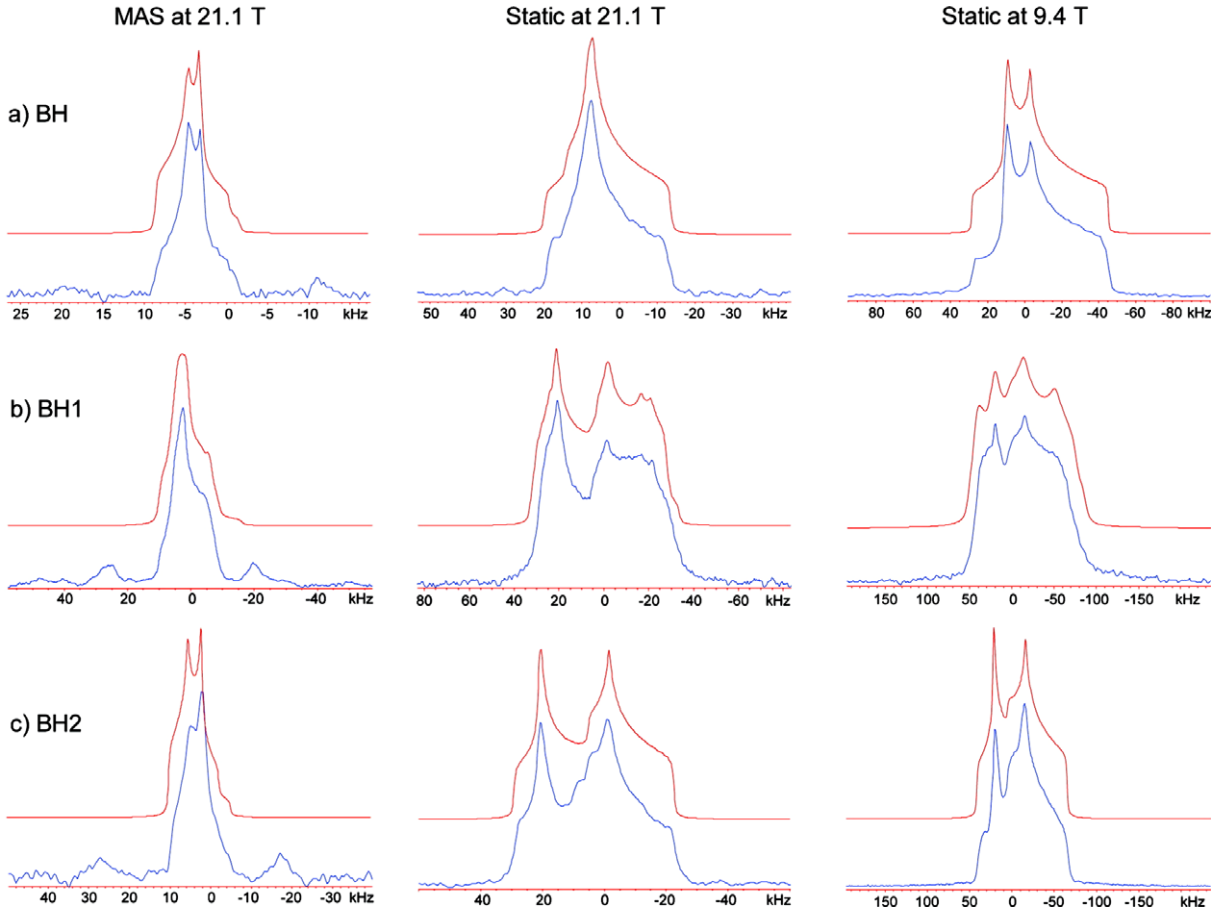

Fig. 13. Chlorine-35 SSNMR spectra at 21.1 and 9.4 T (bottom) and simulations (top) of monohydrated bupivacaine HCl (BH) polymorphs: (a) commercial BH; (b) BH1 obtained by heating BH to 120 °C; (c) BH2 obtained by heating BH to 170 °C. From H. Hamaed, J.M. Pawlowski, B.F.T. Cooper, R. Fu, S.H. Eichhorn and R.W. Schurko, J. Am. Chem. Soc. 130 (2008), 11056. Reproduced by permission of the American Chemical Society.

chemical shifts of −127.6 and −124.6 ppm (referenced to 1 M NaCl(*aq*)).

5. Bromine-79/81 experimental data

Compared to chlorine, significantly less SSNMR data are available for $^{79/81}$Br, despite the higher receptivity of the latter nuclides. This is the result of the larger Q values for the $^{79/81}$Br nuclei, which often renders the collection of bromine SSNMR spectra difficult. However, the increased availability of high magnetic fields will likely lead to more bromine SSNMR studies. In addition, the improvement in accuracy, and increased availability, of quantum chemical computational software will likely also aid researchers, as calculations provide a method of predicting which materials will have C_Q values small enough to be characterized in a given magnetic field.

5.1. Simple cubic bromides

The simple cubic salts of bromine have been widely studied by SSNMR, due to the absence of any significant QI at the bromine nucleus. For bromine, the vast majority of published studies examine salts in which the bromine sits in a site where the surrounding EFG is nearly zero. The data for simple inorganic bromide salts are summarized in Tables 2 and 8.

Many of the initial chlorine SSNMR studies included bromine and iodine as well. Interestingly, Pound carried out the first bro-

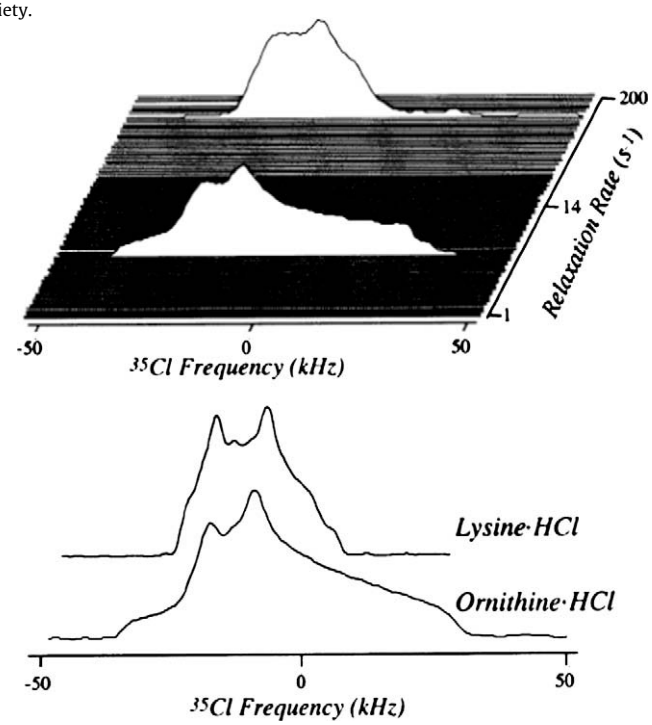

Fig. 14. Top: two-dimensional RAS spectroscopy of CT ^{35}Cl powder patterns for a mixture of lysine HCl and ornithine HCl at 14.1 T [89]. The corresponding one-dimensional spectra for pure samples are shown below. From Lupulescu et al. J. Am. Chem. Soc. 125 (2003), 3376. Reproduced by permission of the American Chemical Society.

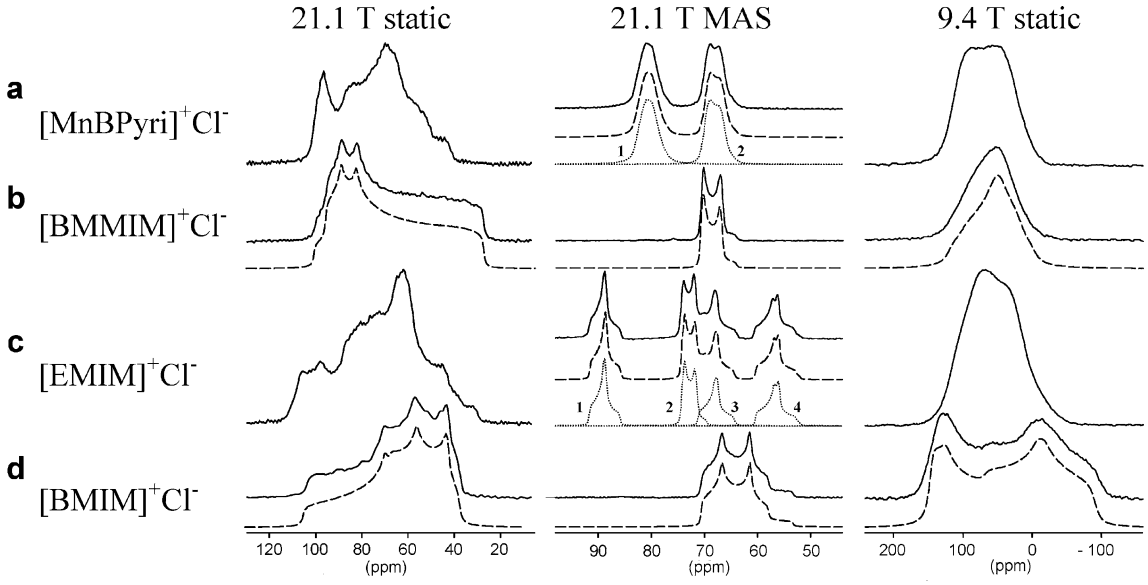

Fig. 15. Chlorine-35 NMR spectra of powdered samples of the chloride salts of: (a) methyl-*N*-butylpyridinium; (b) butyldimethylimidazolium; (c) ethylmethylimidazolium; (d) butylmethylimidazolium. Dashed lines are best-fit simulated spectra. From P.G. Gordon, D.H. Brouwer, J.A. Ripmeester, J. Phys. Chem. A 112 (2008) 12527. Reproduced by permission of the American Chemical Society.

mine-79/81 SSNMR study on a single crystal of NaBr in 1950, years before Kanda studied the ^{35}Cl nucleus [71,104]. Shortly thereafter, Pound and Watkins carried out experiments on KBr single crystals, concluding that the EFG surrounding the bromine nucleus was actually not exactly zero, as a result of lattice imperfections [105,106]. The authors attributed these imperfections to lattice

Table 6
Selected chlorine-35 quadrupolar parameters and isotropic chemical shifts for perchlorates.[a]

Compound	δ_{iso}/ppm	$C_Q(^{35}Cl)$/MHz	η_Q	References
$NaClO_4$	1044.3(0.5)[b]	0.887(0.014)	0.92(0.02)	Skibsted and Jakobsen [70]
$NaClO_4 \cdot H_2O$	1039.9(0.3)[b]	0.566(0.009)	0.90(0.02)	Skibsted and Jakobsen [70]
	1040.1(0.5)[c]	0.459(0.012)[c]	0.91(0.04)[c]	
NH_4ClO_4	917.5(0.7)[d]	0.6949(0.0005)	0.7552(0.0012)	Bastow and Stuart [97]
	–	0.640(0.040) (300 K)	0.80(0.10)	Segel et al. [96]
	930[d]	–	–	Bastow et al. [97]
$LiClO_4$	1034.2(0.5)[b]	1.282(0.008)	0.34(0.01)	Skibsted and Jakobsen [70]
	1034.1(0.5)[c]	1.010(0.012)[c]	0.34(0.01)[c]	
$LiClO_4 \cdot 3H_2O$	1045.9(0.5)[b]	0.695(0.004)	0.00(0.03)	Skibsted and Jakobsen [70]
$KClO_4$	–	0.51(0.01) (296 K)	0.52(0.10)	Tarasov et al. [99]
	1049.2(0.3)[b]	0.440(0.006)	0.88(0.02)	Skibsted and Jakobsen [70]
$RbClO_4$	−3(5)[e]	~0.6	0.53(0.02)	Tarasov et al. [99]
	1049.4(0.3)[b];	0.537(0.015)	0.87(0.03)	Skibsted and Jakobsen [70]
	1049.1(0.3)[c]	0.424(0.014)[c]	0.86(0.02)[c]	
$CsClO_4$	–	~0.63	0.55	Tarasov et al. [98]
	1047.7(0.3)[b]	0.585(0.008)	0.86(0.02)	Skibsted and Jakobsen [70]
$Mg(ClO_4)_2$	1036.2(0.5)[b]	2.981(0.007)	0.57(0.01)	Skibsted and Jakobsen [70]
$Mg(ClO_4)_2 \cdot 6H_2O$	site 1: 1046.6(0.3)[b]	site 1: 0.309(0.006)	0.00(0.08)	Skibsted and Jakobsen [70]
	1046.6(0.3)[c]	0.245(0.005)[c]	0.00(0.10)[c]	
	site 2: 1045.5(0.3)[b]	site 2: 0.475(0.008)	0.00(0.05)	
	1045.5(0.3)[c]	0.375(0.003)[c]	0.00(0.07)[c]	
$Ba(ClO_4)_2$	1029.6(0.5)[b]	2.256(0.008)	0.58(0.01)	Skibsted and Jakobsen [70]
$Ba(ClO_4)_2 \cdot 3H_2O$	1040.6(0.3)[b]	0.383(0.005)	0.00(0.03)	Skibsted and Jakobsen [70]
	1040.5(0.5)[c]	0.299(0.004)[c]	0.01(0.03)[c]	
$Cd(ClO_4)_2 \cdot 6H_2O$	1044.4(0.3)[b]	0.328(0.005)	0.00(0.03)	Skibsted and Jakobsen [70]
$(CH_3)_4NClO_4$	1049.3(0.3)[b]	0.307(0.004)	0.00(0.03)	Skibsted and Jakobsen [70]
Trimethylammonnium perchlorate	–	Phase III: 370 kHz Phase II: 318 kHz	Phase III: 0.60–1.0	Jurga et al. [95]
Dimethylammonnium perchlorate	Phase I: 1003[f]	Phase III: 1.120 Phase II: 0.238	Phase III: 0 Phase II: 0	Jurga et al. [95]
Monomethylammonium perchlorate	–	Phase III: 1.016 Phase II: 0.258	Phase III: 0.75 Phase II: 0	Jurga et al. [95]

[a] Errors are given in parentheses.
[b] With respect to NaCl(*s*).
[c] Refers to ^{37}Cl value.
[d] With respect to $NH_4Cl(s)$.
[e] With respect to 0.1 M $RbClO_4(aq)$.
[f] With respect to KCl(*s*).

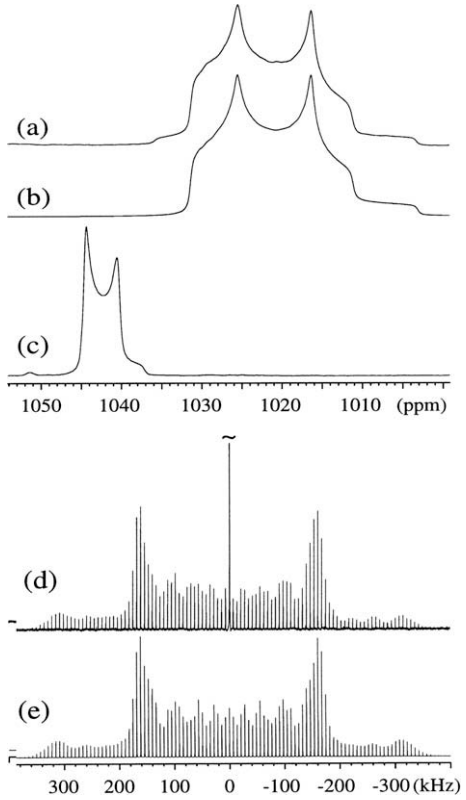

Fig. 16. (a) ^{35}Cl MAS NMR spectrum at 14.1 T of the CT for $LiClO_4$ (ν_r = 8.0 kHz) and (c) $LiClO_4 \cdot 3H_2O$ (ν_r = 7.0 kHz). (b) Simulation of the second-order quadrupolar line shape for $LiClO_4$. (d) ^{35}Cl MAS NMR spectrum at 14.1 T of the STs for $LiClO_4 \cdot 3H_2O$ (ν_r = 7.0 kHz) shown with the CT cut off at approximately $^1/_8$ of its total height. (e) Simulation of the ssb manifold in (d), employing the optimized NMR parameters for $LiClO_4 \cdot 3H_2O$. From Skibsted and Jakobsen, Inorg. Chem. 38 (1999), 1806. Reproduced by permission of the American Chemical Society.

dislocations and the resulting QI 'smeared' the satellite transitions over a large spectral width, resulting in a decrease in the signal intensity.

Kanda, Yamagata, and Hayashi and Hayamizu all included bromine NMR in their studies of simple halide salts and noted the same trends that were observed for the chlorides [71,72,74]. Many of the experiments mentioned for the chlorine cubic salts, such as examining the temperature and pressure dependence of T_1 and the effect of elastic strain on the CT, were also carried out for $^{79/81}$Br [81,107–111]. In addition, there are many studies which monitored the effects of doping on the CT bromine NMR signal (as well as the diffusion of the impurities) of cubic bromide salts, which yielded the expected result that dopants decrease the intensity and increase the line width of the bromine CT [112–116]. An additional study looked at dislocation effects and how they influenced bromine self-diffusion in a freshly prepared sample of AgBr [117].

The ^{79}Br NMR spectrum of KBr powder collected under MAS conditions features a large manifold of spinning sidebands due to the $^{79/81}$Br STs. This manifold was found to be extremely sensitive to slight changes in the magic angle setting. For this reason, it was proposed by Frye and Maciel that the ^{79}Br NMR spectrum of powdered KBr be used to set the magic angle [118]. As bromine-79 is actually quite receptive, and the cubic symmetry of KBr results in very minimal quadrupolar broadening, a reasonable spectrum can be collected in a single scan. In addition, the proximity of the resonance frequency of ^{13}C to that of ^{79}Br makes the sample a convenient choice with regards to probe tuning. The ^{79}Br chemical shift and T_1 in KBr have also been proposed to be used for temperature measurement in NMR samples over the range 20–320 K [119], echoing an earlier suggestion of using the ^{81}Br signal of KBr to measure inhomogeneous temperature distributions in MRI experiments [120].

5.2. Perbromates

The experimental data resulting from bromine-79/81 SSNMR studies of perbromates are given in Table 9. Analogously to the perchlorates, in these perbromates the bromine sits at a position of relatively high symmetry. To the best of our knowledge, there are three studies of these materials, all carried out by Tarasov et al. [121] In these studies, four perbromate powders were examined: $KBrO_4$, $RbBrO_4$, $CsBrO_4$, and NH_4BrO_4. All four materials were studied under static conditions (see Fig. 17 for an example). Quadrupolar coupling constants and asymmetry parameters were reported; the largest $C_Q(^{81}Br)$ observed was 3.35 ± 0.03 MHz for $KBrO_4$. The authors did not consider CSA in their fits. The symmetry of the systems suggests that CSA will be small, but nonzero. It would be interesting to systematically re-examine a series of perbromates in much stronger magnetic fields, in order to obtain some information on bromine CSA and how it relates to structure.

5.3. Other materials

The experimental $^{79/81}$Br SSNMR data available for other bromine-containing systems are summarized in Table 10. Unlike the hydrochlorides, the hydrobromides have not been widely studied using SSNMR, with only three examples in the literature to the best of our knowledge. The two most recent examples were reported in a 2007 paper by Persons and Harbison, in which they used samples of leucine HBr and tyrosine HBr to demonstrate their STREAQI method, as described in Section 3.1 (Fig. 18) [63]. Bromine-79 C_Q values of 49.0 and 11.26 MHz were reported for L-leucine HBr and L-tyrosine HBr, respectively. Bromine CSA was not included quantitatively in the analysis; however, the authors observed the qualitative effects of CSA, particularly in the spectrum of L-tyrosine HBr.

Two alkaline earth metal bromide type systems have been studied by ^{81}Br SSNMR: Tris–sarcosine $CaBr_2$ [122] and $BaBr_2$ [123]. A single crystal of tris-sarcosine $CaBr_2$ was analyzed by Erge et al. in 1991 and a $C_Q(^{81}Br)$ value of 21.9 MHz (η_Q = 0.64) was determined. These values may be compared to $C_Q(^{35}Cl)$ = 4.04 MHz and η_Q = 0.62 for Tris–sarcosine $CaCl_2$ [53]. On the basis of the product of the quadrupole moment and Sternheimer antishielding factor for the two nuclei, it is possible to predict that the ratio between $C_Q(^{81}Br)$ and $C_Q(^{35}Cl)$ should be 6.11 if the two compounds are isostructural. This is slightly higher than the experimental value of 5.42. The remaining discrepancy is likely attributable to the different unit cell sizes, as demonstrated by Wu and Terskikh for the alkali metal NMR parameters in a series of alkali metal tetraphenylborates [28].

Trill et al. also included several bromine-containing sodalites in their SSNMR studies of mixed halogen sodalite systems [124]. The bromine-81 quadrupolar products, P_Q, were found to range from 0.3 to 0.7 MHz for the mixed Cl–Br sodalites, and from 0.3 to 1.0 MHz for mixed I–Br samples. Similar to the conclusion reached for chlorine, a linear correlation between $\delta(^{81}Br)$ and the M–Br bond distance was noted.

6. Iodine-127 experimental data

There are comparatively few ^{127}I SSNMR data in the literature, due in large part to its large Q (Table 1). Although it is likely that increased field strengths will lead to an increase in the number

Table 7
Selected chlorine-35 quadrupolar parameters and isotropic chemical shifts for sodalites, glasses, and other materials.[a]

Compound	δ_{iso}/ppm	$C_Q(^{35}Cl)$/MHz	η_Q	References
Mixed Cl/Br sodalites (varied from 5% Cl to 100% Cl)	−125.4(0.2)[b] (5% Cl)–123.2(0.2) (100% Cl)	P_Q[c] = 0.2(0.1) for all Cl percentages; P_Q = 55(5) kHz for pure chloro-sodalite		Trill et al. [46]
Mixed Cl/I sodalites (varied from 5% Cl to 100% Cl)	−128.2(0.3)[b] (5% Cl)–123.2(0.3) (100% Cl)	P_Q = 0.2(0.1) for all Cl percentages from MAS		Trill et al. [46]
Several Cl-containing silicate and aluminosilicate glasses[e]				
Silicates				
NS	−65(5)[d]	3.3(0.1)	0.7[e]	Sandland et al. [85]
N2CS	−67(10)[d]	3.0(0.2)		
CNS	−35(15)[d]	3.2(0.4)		
C2NS	−20(15)[d]	3.3(0.3)		
CS	102(22)[d]	4.4(0.4)		
Alumino-silicates				
NAS1	−89(11)[d]	3.0(0.3)		
NAS4	−65(7)[d]	2.9(0.2)		
CAS1	52(38)[d]	3.5(0.9)		
CAS3	62(45)[d]	3.6(1.0)		
CAS4	79(42)[d]	4.0(0.9)		
$Mg_3Al(OH)_6ClO_4 \cdot nH_2O$	1001.2[d] (0% RH)	–	–	Hou and Kirkpatrick[133]
$LiAl_2(OH)_6Cl \cdot nH_2O$ (“LiAlCl5”; “LiAlCl6”; “LiAlCl8”)	Spectra recorded at several relative humidities (RH) and temperatures. 8.97[d] (0% RH)	0.9 (room humidity and temperature)	0	Hou et al.[131,132]
Coal A	−49.6[f] peak assigned to NaCl	–	–	Saito et al.[144]
$(CH_3)_4NCdCl_3$	–	Phase I (296 K): 13.48 phase I (120 K): 13.64 phase II (115 K): site 1: 14.98 site 2: 14.02 site 3: 12.64 phase III (98 K): site 1: 15.18 site 2: 14.72 site 3: 14.68 site 4: 13.98 site 5: 13.90 site 6: 13.86 site 7: 13.52 site 8: 13.30 site 9: 13.04	Phase I (296 K): 0.16 phase I (120 K): 0.13 phase II, site 1: 0.12 phase II, site 2: 0.22 phase II, site 3: 0.27	Mulla-Osman et al. [145–147]
$YBa_2Cu_3O_{6.7}Cl_{0.2}$ (Cl-doped YBCO)	–	∼2	1	Goren et al. [148]
Hydrotalcite	–	∼2.4 (176 K) ∼1.5 (233 K) ∼1.2 (room temp)	∼1 ∼0 –	Kirkpatrick et al. [149]
Hydrocalumite	30(5)[g] (283–403 K) 26(5)[g] (<273 K)	2.87 (283 K) 2.22 (403 K) 3.0 (<273 K)	∼0 ∼0 0.9	Kirkpatrick et al. [149]
$CH_3NH_3GeCl_3$	–	∼25 (low temp); → 0 (500 K)	–	Yamada et al. [150,151]
Cl-doped yttrium ceramics (YBCO-Cl)	–	site 1: 1.2 site 2: 1.4 site 3: 1.9	–	Amitin et al. [152]
Calcium chloroapatite	–	0.8	–	Yesinowski and Eckert [86,153]
p-dichlorobenzene	–	73.96	0.0712(0.0005)	Creel et al. [134]
$Ca_{4.99\text{-}5.06}(PO_4)_{2.98\text{-}3.00}F_{0.51\text{-}0.48}Cl_{0.38\text{-}0.36}OH_{0.14\text{-}0.12}$	∼115[d]	∼1.6	–	McCubbin et al. [154]
$(CH_3)_2CHNH_3CuCl_3$	–	site 1: 19.5 site 2: 25.17 site 3: 21.05	0.68 0.5 0.58	Saito et al. [155]

[a] Errors are given in parentheses.
[b] With respect to 1M NaCl(*aq*).
[c] $P_Q = C_Q(1 + \eta_Q^2/3)^{1/2}$.
[d] With respect to 1 M NaCl(*aq*).
[e] C_Q was determined with η_Q arbitrarily set to 0.7. Estimated mean values of C_Q could therefore vary by up to 15%. See Sandland et al. [85] for explanations of labels for silicates and aluminosilicates.
[f] With respect to KCl(*s*).
[g] No chemical shift reference given.

of iodine SSNMR reports, we expect that the studies will remain limited to systems where the iodine sits in a relatively high-symmetry environment. As with bromine, quantum chemical calculations will play an important role, allowing researchers to fairly

Table 8
Chlorine, bromine, and iodine quadrupolar coupling constants and isotropic chemical shifts for simple inorganic halides.[a]

compound	δ_{iso}/ppm	$C_Q(^{81}Br)$/MHz	References
NH_4Cl	74.0[b]	–	Weeding and Veeman [73]
	73.8[b] (^{37}Cl)		
NaCl	−46.1[b]	–	Weeding and Veeman [73]
	−42.0[b] (^{37}Cl)		
NaCl/cement	~30[c]	–	Barberon et al. [156]
KCl	3.07[b]		
	2.8[b] (^{37}Cl)	–	Weeding and Veeman [73]
RbCl	44.7[b]	–	Weeding and Veeman [73]
	44.8[b] (^{37}Cl)		
CsCl	109.4[b]	–	Weeding and Veeman [73]
	109.6[b] (^{37}Cl)		
CuCl	−127.23(0.05)[d]	–	Hayashi and Hayamizu [69]
AgCl	−12.82(0.05)[d]	–	Hayashi and Hayamizu [69]
TlCl	−250[e]	–	Guenther and Hultsh [157]
AgBr	169.35(0.07)[f]	–	Hayashi and Hayamizu [69]
	208[g]	–	Jelinek et al. [158]
TlBr	620(50)[h]	–	Kanda [71]
NH_4Br			
Phase II	233(10)[i]	–	Itoh and Yamagata [159,160]
Phase I	132(10)[i]	–	
Phase III	–	5.5(0.3)	
	–	5.656(0.01)	Jeffrey et al. [161]
CuBr	−116(10)[j]	–	Günther and Hultsch [157]
	−134.14(0.2)[f]	–	Hayashi and Hayamizu [69,162]
CuI	7.7(0.2)[k]	–	Hayashi and Hayamizu [69]
AgI	−230.2(1.0)[k]	–	Hayashi and Hayamizu [69]

[a] Errors are given in parentheses. Precise data for alkali metal halides are provided in Table 2. Data are for ^{35}Cl, ^{81}Br, and ^{127}I unless otherwise indicated.
[b] With respect to infinitely dilute Cl^-.
[c] With respect to NaCl(*aq*); concentration not specified.
[d] With respect to KCl(*s*).
[e] With respect to saturated NaCl(*aq*).
[f] With respect to KBr(*s*).
[g] With respect to 0.1 M NaBr(*aq*).
[h] With respect to NaBr(*aq*).
[i] With respect to a dilute aqueous alkali bromide solution.
[j] With respect to saturated NaBr(*aq*).
[k] With respect to KI(*s*).

Table 9
Bromine-81 quadrupolar parameters and isotropic chemical shifts for solid perbromates.[a]

Compound	δ_{iso}/ppm[b]	$C_Q(^{81}Br)$/MHz	η_Q	References
$KBrO_4$	–	3.35(0.03)	0.71(0.05)	Tarasov et al. [163]
$RbBrO_4$	–	2.36(0.04)	0.37	Tarasov et al. [163]
$CsBrO_4$	2400(200)	1.32(0.04)	0	Tarasov et al. [121]
		1.53(0.06)[d]		
NH_4BrO_4	2440(120)	2.27(0.05)	0.99	Tarasov et al. [164]
	2500(130)[c,d]	2.72(0.05)[d]		
	–	2.38(0.03)	0.91	Tarasov et al. [163]

[a] Errors are given in parentheses.
[b] With respect to 1 M KBr(*aq*).
[c] Shift reference not given.
[d] Data for ^{79}Br.

accurately predict whether an iodine SSNMR experiment is feasible at a given field strength.

6.1. Simple cubic iodides

Selected experimental data for simple iodides are summarized in Tables 2 and 8. The high symmetry in these materials has allowed them to be relatively widely studied. The first iodine SSNMR study appears to have been carried out on a single crystal of KI [104]. In addition, ^{127}I SSNMR experiments on KI yielded the same result that was noted in the potassium bromide case – namely that

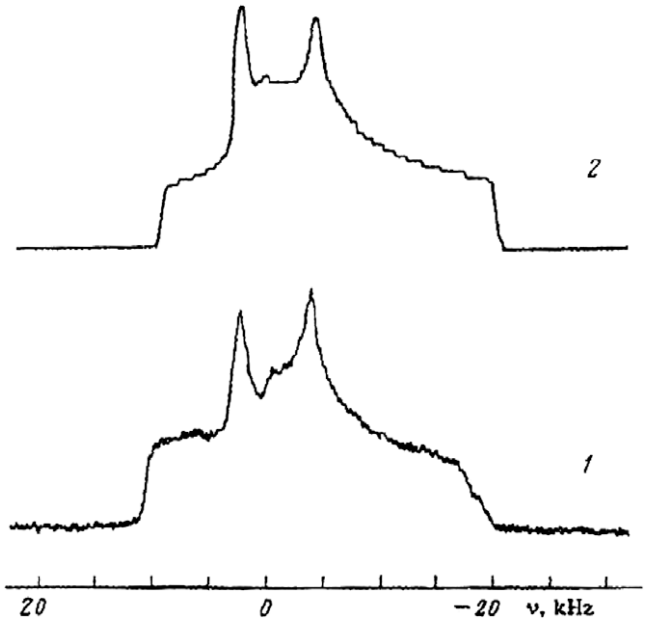

Fig. 17. Bromine-81 CT NMR spectra for powdered $KBrO_4$ collected under static conditions (T = 297 K, ν_0 = 81.256 MHz). Bottom: experimental; top: simulation. From V.P. Tarasov, V.I. Privalov, K.S. Gavrichev, V.E. Gorbunov, Yu. K. Gusev, Yu. A. Buslaev, Russ. J. Coord. Chem. 16 (1990), 854. Copyright Plenum Press. Reproduced with kind permission of Springer Science and Business Media.

the EFG about the iodine site was not perfectly zero due to lattice vibrations/dislocations [105,106].

Simple iodides were included in some of the SSNMR studies of cubic halogens described previously, such as the reports of Kanda, Yamagata, and Hayashi and Hayamizu [71,72,74]. In the MAS study of Hayashi and Hayamizu, the iodine-127 chemical shift trend was only partially consistent with the results for bromine and chlorine. Their results found the shift trend to be CsI > LiI > RbI > NaI > KI, which is inconsistent with trends in ionic radius or cation electronegativity [74].

In a detailed multinuclear magnetic resonance study of a series of silver halides, AgX (X = F, Cl, Br, and I), the authors used ^{19}F, ^{35}Cl, ^{81}Br, ^{127}I, and ^{109}Ag SSNMR experiments to comment upon the temperature dependence of the observed chemical shifts [125]. It was demonstrated that the overlapping ion theory, then commonly used to model observed shifts, failed to predict the anion chemical shifts of the quadrupolar halogens, while the silver shifts were in good agreement.

6.2. Periodates

Along with the simple iodides, the periodates make up the majority of iodine SSNMR data available in the literature; the experimental data available for these systems are presented in Table 11. The first of these studies was published by Segel and Vyas in 1980 and reported ^{127}I C_Q values for four periodates: NH_4IO_4, KIO_4, $AgIO_4$, and $NaIO_4$ [126]. The C_Q values were found to range from 10.02 MHz for NH_4IO_4 to 42.39 MHz for $NaIO_4$. The CS tensors were also examined in this study with some surprisingly large spans reported, the highest being 59,000 ppm. No NMR spectra, however, were shown in this publication.

In 2001, Wu and Dong revisited the ^{127}I SSNMR spectroscopy of selected periodates (HIO_4, NH_4IO_4, KIO_4, $AgIO_4$, and $NaIO_4$) [127]. The authors noted that the very large CS tensor spans reported by Segel and Vyas [126] for $NaIO_4$ seemed suspect due to the symmetry in the system, and then demonstrated that the CSA was actually less than 50 ppm for all five periodates. An exact

Table 10
Selected bromine-81 quadrupolar parameters and isotropic chemical shifts for sodalites, organic hydrobromides, and other materials.[a]

Compound	δ_{iso}/ppm	$C_Q(^{81}Br)$/MHz	η_Q	References
Mixed Cl/Br sodalites (varied from 10% to Br to 100% Br)	−220.6(0.4)[b] to −217.3(0.4)	P_Q[c] = 0.7(0.2)–0.3(0.2)		Trill et al. [46]
Mixed Br/I sodalites (varied from 6% to Br to 100% Br)	−226.4(0.4)[b] to −220.6(0.4)	P_Q = 0.3(0.2)–1.0(0.2)		Trill et al.[46]
$Na_8[Al_6Si_6O_{24}]Br_n\cdot(H_3O_2)_{2-n}$ (varied from n = 0.98−0.10)	−221.0[b] to −218.0	P_Q = 0.5–0.8		Trill et al.[124]
$Na_{6+n}[Al_6Si_6O_{24}]Br_n\cdot(4H_2O)_{2-n}$ (varied from n = 0.98−0.10)	−221.0[b] to − 230.6	P_Q = 0.5–2.2		Trill et al. [124]
$Na_{6+n}[Al_6Si_6O_{24}]Br_n\cdot\varphi_{2-n}$ (φ = empty sodalite cage) (varied from n = 0.98−0.10)	−221.0[b] to −237.8	P_Q = 0.5–1.0		Trill et al. [124]
$Na_8[Al_6Si_6O_{12}]Br_2$	-219[f]	–	–	Jelinek et al. [158,165]
$Na_{8-n-p}Ag_n[Si_6Al_6O_{12}]Br_{2-p}$ (various n and y)	−219/−550[f]	–	–	Jelinek et al. [158,165]
$Ag_8[Al_6Si_6O_{12}]Br_2$	−550[f]	–	–	Jelinek et al. [158,165]
$K_2Pt(CN)_4Br_{0.3}\cdot 3.2\ H_2O$				
I	–	17.6	0	Brenni et al. [166]
II	–	15.1	0	Brinkmann et al. [167]
BaFBr:O (2%)	–	10.00	0	Bastow et al. [141]
C_n–DABCO–C_n–Br_2 (n = 10,12, and 14) (DABCO = 1,4-diazoniabicyclo[2.2.2]octane)	3660[d,e]	–	–	Nakayama et al. [168]
Tris–sarcosine $CaBr_2$	–	21.9	0.64	Erge et al. [122]
$BaBr_2$	–	–	–	Potrepka et al. [123]
$C_{60}Br_{24}Br_2$	–	–	–	Milia et al. [169,170]
Deuterated glycyl-L-alanine HBr · H_2O	–	19.750	0.8328	Kehrer et al. [171]
L-leucine HBr	–	49.0[e]	0.59	Persons and Harbison [63]
L-tyrosine HBr	–	11.26[e]	0.86	Persons and Harbison [63]

[a] Errors are given in parentheses.
[b] With respect to 1 M NaBr(*aq*).
[c] $P_Q = C_Q(1 + \eta_Q^2/3)^{1/2}$.
[d] With respect to NaBr(*s*).
[e] Data for ^{79}Br.
[f] With respect to 0.1 M NaBr(aq).

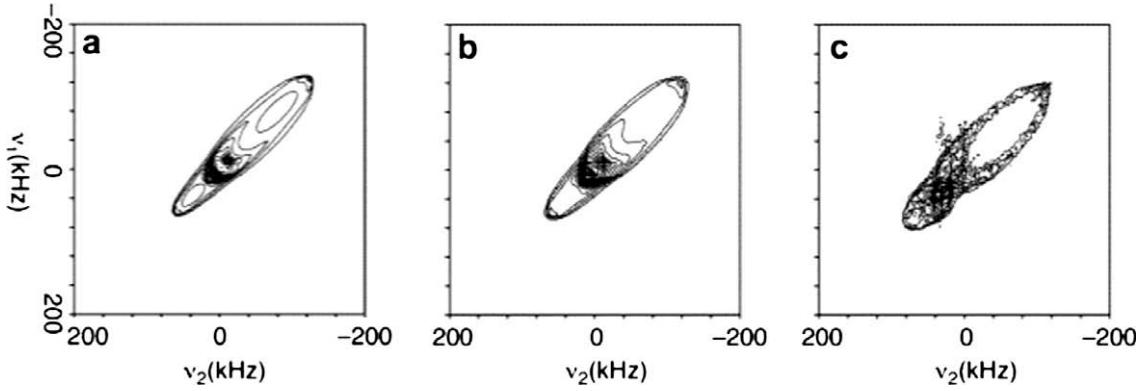

Fig. 18. ^{79}Br STREAQI NMR spectra of L-tyrosine HBr at 14 T, simulated using the assumption (a) of a discrete jump of the rotor between two static orientations and (b) continuous sample rotation; compared with (c) an experimental spectrum. From J. Persons and G.S. Harbison, J. Magn. Reson. 186 (2007) 347. Reproduced by permission of Elsevier Limited.

value of 18 ppm was determined for $CsIO_4$ [127]. This remains as what is likely the only reliable iodine CS tensor span determined by SSNMR spectroscopy.

The ^{127}I C_Q in several periodates was shown to be highly dependent on temperature in a series of studies by Burkert and co-workers in the 1980s [128]. For example, in the case of NH_4IO_4, C_Q was found to vary from 1.31 to 11.59 MHz over the temperature range 145–440 K [128]. A consistent relationship was not found amongst different periodates however, as the C_Q value increased with increasing temperature in some cases, while decreasing in others [128].

6.3. Other materials

The available iodine SSNMR data for other materials are summarized in Table 11. Few materials other than simple iodides and periodates have been studied. However, in a 1970 study done at 0.936 T, polycrystalline $IF_6^+AsF_6^-$ was examined by ^{127}I SSNMR, which was feasible due to the fairly symmetric environment about the iodine nucleus in the cation [129]. The authors were able to determine that the iodine-127 C_Q value was between 2.32 and 2.9 MHz. In addition, Trill et al. have also used ^{127}I SSNMR to study several mixed halogen sodalite systems at 11.7 T [46]. The authors determined that the ^{127}I quadrupolar products in the mixed Cl–I sodalite systems varied from 1.0 to 3.9 MHz and from 1.0 to 2.8 MHz in the mixed Br–I sodalites.

7. Outlook and conclusions

Significant advances in the application of $^{35/37}$Cl solid-state NMR spectroscopy, and the interpretation of the results in terms of local structure, have occurred in the past few years. The majority of recent studies have understandably focused on chloride ions in

Table 11
Iodine-127 quadrupolar parameters and isotropic chemical shifts for periodates and other materials.[a]

compound	δ_{iso}/ppm	$C_Q(^{127}I)$/MHz	η_Q	references
KIO_4	3960(10)[b]	20.66(0.01)	0	Wu and Dong [127]
	6530(200)[c]	20.73	–	Segel and Vyas [126]
NH_4IO_4	3960(10)[b]	10.00(0.01)	0	Wu and Dong [127]
	–	1.31–11.59 (145–440 K)	–	Burkert [128]
	3810(50)[c]	10.02	–	Segel and Vyas [126]
$RbIO_4$	3960(10)[b]	15.65(0.01)	0	Wu and Dong [127]
	–	16.27–14.65 (202–433 K)	–	Burkert [128]
$NaIO_4$	3950(10)[b]	42.24(0.01)	0	Wu and Dong [127]
	−5370(100)[c]	42.39	–	Segel and Vyas [126]
$CsIO_4$	3972(2)[b]	1.00(0.01)	0	Wu and Dong [127]
	–	11.45–10.45 (202–294 K); 1.8–1.7 (300–315 K)	–	Burkert [128]
HIO_4	3300(10)[b]	43.00(0.01)	0.75	Wu and Dong [127]
$(CH_3)_4AsIO_4$	–	$\leqslant$1.8	–	Grommelt and Burkert [172]
$(n\text{-}C_4H_9)_4PIO_4$	–	5.98–3.14 (150–355 K)	0.08 to 0.30	Burkert and Grommelt [32]
$(C_2H_5)_4SbIO_4$	–	5.29–5.71 (217–301 K)	0.64 to 0.38	Klobasa and Burkert [173]
$(C_2H_5)_4PIO_4$	–	6.09–5.87 (177–302 K)	–	Klobasa et al. [174]
$(C_2H_5)_4AsIO_4$	–	5.82–5.55 (197–299 K)	–	Klobasa et al. [174]
$(C_6H_5)_4PIO_4$	–	4.12–5.71 (228–293 K)	~0	Burkert and Klobasa; Klobasa et al. [174,175]
$(C_6H_5)_4AsIO_4$	–	3.50–7.42 (179–297 K)	~0	Burkert and Klobasa; Klobasa et al. [174,175]
$(C_6H_5)_4SbIO_4$	–	1.37–2.76 (228–302 K)	~0	Burkert and Klobasa; Klobasa et al. [174,175]
$(CH_3)_4NIO_4$	–	20–15 (200–300 K)	–	Klobasa and Burkert [173]
$(n\text{-}C_4H_9)_4NIO_4$	–	8.07–3.35 (225–310 K)	0.60 to 0.77	Burkert and Grommelt [32]
$N(CH_3)_4IO_4$	–	15.46–9.07 (301–418 K)	–	Burkert [128]
$AgIO_4$	5410(50)[c]	29.66	–	Segel and Vyas [126]
Mixed Br/I sodalites (varied from 0% Br–90% Br)	−255.5(0.8)[d] to −245.0(0.8)	P_Q[e] = 1.0(0.5)–2.8(0.5)		Trill et al. [46]
Mixed Cl/I sodalites (varied from 0% Cl–90% Cl)	−255.5(0.8)[d] to −227.1(0.8)	P_Q = 1.0(0.5)–4.3(0.5)		Trill et al. [46]
IF_7	3040(40)[f]	134.88(0.03) (77 K)	0.04(0.004)	Weulersse et al. [176]
$IF_6^+AsF_6^-$	–	2.9–2.32	–	Hon and Christe [129]
$Mn(CO)_5I$	–	927	0.03	Spiess and Sheline [137]

[a] Errors are given in parentheses.
[b] With respect to KI(*s*).
[c] With respect to NaI(*s*).
[d] With respect to 1 M KI(*aq*).
[e] $P_Q = C_Q(1 + \eta_Q^2/3)^{1/2}$.
[f] With respect to 5 M KI(*aq*).

various organic and inorganic environments, due to the relatively small QI of the chloride nucleus. This article has highlighted what we believe to be the most important recent developments, e.g., the interpretation of $^{35/37}$Cl quadrupolar and CS tensors in organic hydrochlorides in terms of hydrogen bonding environment; the demonstration of the sensitivity of $^{35/37}$Cl SSNMR to polymorphism and pseudopolymorphism in materials ranging from pharmaceutical hydrochlorides to inorganic chlorides; the characterization of solid ionic 'liquids' via chlorine SSNMR. Covalently bound chlorine presents more of a challenge for modern SSNMR methods, particularly for chlorine bound to carbon, where the value of $C_Q(^{35}Cl)$ typically exceeds 70 MHz [13,82]. However, when chlorine is covalently bound to transition metals, it has been shown that the observed $C_Q(^{35}Cl)$ are much smaller [52]. Overall, it is seen that ultrahigh magnetic field strengths ($\geqslant$18.8 T) have been extremely beneficial to the above-mentioned studies. By and large, it is clear that the $^{35/37}$Cl nuclides will remain the most accessible to study by SSNMR, and it is for these nuclides that the most comprehensive understanding of the relationship between local structure and the observed NMR spectrum is available. We anticipate continued advances in this area, with further applications to a range of systems comprising organic, biomolecular, inorganic, and organometallic compounds.

New developments in the field of $^{79/81}$Br and ^{127}I SSNMR spectroscopy have been scarce due to the large quadrupole moments and Sternheimer antishielding factors associated with these nuclei. Nevertheless, for the bromine nuclides in particular, ultrahigh magnetic fields should create new opportunities for study. Variable-offset approaches will likely be required to make progress. Potential alternatives include the STREAQI and WURST approaches [58,59,63]. Regardless of the method used, there is still work to be done to build a better understanding of the structural and electronic factors which influence the quadrupolar and shielding interactions for $^{79/81}$Br and ^{127}I. For example, there is essentially no information concerning bromine CS tensors, with a report by Fusaro and Doane being the lone exception [130] in solids, and only one reliable report for ^{127}I [127]. Therefore, while the spectroscopy will remain challenging due to large second-order quadrupolar broadening for all but the most symmetric of environments, there is also a great deal of room for development and exploration in this area of NMR spectroscopy.

Acknowledgements

D.L.B. thanks the Natural Sciences and Engineering Research Council (NSERC) of Canada for funding. C.M.W. thanks NSERC for an Alexander Graham Bell CGS D2 scholarship. We are grateful to Aaron Rossini and Prof. Rob Schurko for providing a preprint of reference [52]. We thank Prof. Gang Wu for helpful discussions. Access to the 900 MHz NMR spectrometer (Fig. 6) was provided by the National Ultrahigh-Field NMR Facility for Solids (Ottawa, Canada), a national research facility funded by the Canada Foundation for Innovation, the Ontario Innovation Trust, Recherche Québec, the National Research Council Canada, and Bruker BioSpin and managed by the University of Ottawa (www.nmr900.ca). NSERC is acknowledged for a Major Resources Support grant.

References

[1] F.M. Ashcroft, Ion Channels and Disease, Academic Press, San Diego, 2000.
[2] M.E. Loewen, G.W. Forsyth, Physiol. Rev. 85 (2005) 1061.
[3] R. Dutzler, E.B. Campbell, M. Cadene, B.T. Chait, R. MacKinnon, Nature 415 (2002) 287.

[4] R. Dutzler, E.B. Campbell, R. MacKinnon, Science 300 (2003) 108.
[5] T.M. Trnka, J.P. Morgan, M.S. Sanford, T.E. Wilhelm, M. Scholl, T.-L. Choi, S. Ding, M.W. Day, R.H. Grubbs, J. Am. Chem. Soc. 125 (2002) 2546.
[6] K. Mikami, M. Terada, H. Matsuzawa, Angew. Chem. Int. Ed. 41 (2002) 3554.
[7] D.L. Bryce, G.D. Sward, Magn. Reson. Chem. 44 (2006) 409.
[8] C.M. Widdifield, R.P. Chapman, D.L. Bryce, Chlorine, bromine, and iodine solid-state NMR spectroscopy, in: G.A. Webb (Ed.), Annual Reports on Nuclear Magnetic Resonance Spectroscopy, vol. 66, Elsevier Ltd, 2009, pp. 195–326.
[9] B. Lindman, S. Forsén, Chlorine, bromine and iodine NMR. Physico-chemical and biological applications, in: P. Diehl, E. Fluck, R. Kosfeld (Eds.), NMR Basic Principles and Progress, vol. 12, Springer-Verlag, Berlin, 1976, pp. 1–360.
[10] B. Lindman, S. Forsén, The halogens – chlorine, bromine and iodine, in: R.K. Harris, B.E. Mann (Eds.), NMR and the Periodic Table, Academic Press, London, 1978, pp. 421–436.
[11] T. Drakenberg, S. Forsén, NATO ASI Ser. Ser. C 103 (1983) 405.
[12] J. Mason, Multinuclear NMR, Plenum Press, New York, 1987.
[13] E.A.C. Lucken, Nuclear Quadrupole Coupling Constants, Academic Press, London, 1969.
[14] A. Abragam, Principles of Nuclear Magnetism, Oxford University Press, New York, 1961.
[15] C.P. Slichter, Principles of Magnetic Resonance, Springer-Verlag, New York, 1990.
[16] K. Schmidt-Rohr, H.W. Spiess, Multidimensional Solid-State NMR and Polymers, Academic Press, San Diego, 1994.
[17] K.J.D. MacKenzie, M.E. Smith, Multinuclear Solid-State NMR of Inorganic Materials, Pergamon, Amsterdam, 2002.
[18] M.J. Duer, Solid-State NMR Spectroscopy, Blackwell Publishing, Oxford, 2004.
[19] M.H. Cohen, F. Reif, Solid State Phys. 5 (1957) 321.
[20] U. Haeberlen, Advances in Magnetic Resonance, Supplement 1, Academic Press, New York, 1976.
[21] J. Mason, Solid State Nucl. Magn. Reson. 2 (1993) 285.
[22] H.W. Spiess, Rotation of molecules and nuclear spin relaxation, in: P. Diehl, E. Fluck, R. Kosfeld (Eds.), NMR Basic Principles and Progress, vol. 15, Springer-Velag, Berlin, 1978, pp. 55–214.
[23] M. Mehring, Principles of High Resolution NMR in Solids, Springer-Verlag, New York, 1983.
[24] J. Herzfeld, A.E. Berger, J. Chem. Phys. 73 (1980) 6021.
[25] G.B. Arfken, Mathematical Methods for Physicists, Academic Press, New York, 1985.
[26] R. Sternheimer, Phys. Rev. 80 (1950) 102.
[27] R. Sternheimer, Phys. Rev. 84 (1951) 244.
[28] G. Wu, V. Terskikh, J. Phys. Chem. A 112 (2008) 10359.
[29] A.D. Bain, beta software, private communication, 2008.
[30] R.K. Harris, E.D. Becker, S.M. Cabral de Menezes, R. Goodfellow, P. Granger, Pure Appl. Chem. 73 (2001) 1795.
[31] J. Blaser, O. Lutz, W. Steinkilberg, Z. Naturforsch. A 27 (1972) 72.
[32] P.K. Burkert, M. Grommelt, Z. Naturforsch. 43b (1988) 1381.
[33] A. Loewnstein, M. Shporer, P.C. Lauterbur, J.E. Ramirez, J. Chem. Soc. Chem. Commun. (1968) 214.
[34] M. Gee, R.E. Wasylishen, A. Laaksonen, J. Phys. Chem. A 103 (1999) 10805.
[35] C.Y. Lee, C.D. Cornwell, Magnetic Resonance and Related Phenomena, Groupement Ampere, Heidelberg, 1976. p. 261.
[36] W. Gauß, S. Gunther, A.R. Haase, M. Kerber, D. Kessler, J. Kronenbitter, H. Kruger, O. Lutz, A. Nolle, P. Schrade, M. Schule, G.E. Siegloch, Z. Naturforsch. A 33 (1978) 934.
[37] J. Kondo, J. Yamashita, J. Phys. Chem. Solids 10 (1959) 245.
[38] J. Itoh, Y. Yamagata, J. Phys. Soc. Jpn. 14 (1959) 225.
[39] R. Baron, J. Chem. Phys. 38 (1963) 173.
[40] D. Ikenberry, T.P. Das, Phys. Rev. 138 (1965) A822.
[41] J. Itoh, Y. Yamagata, J. Phys. Soc. Jpn. 13 (1958) 1182.
[42] D.L. Bryce, R.E. Wasylishen, Acc. Chem. Res. 36 (2003) 327.
[43] M.A.M. Forgeron, R.E. Wasylishen, G.H. Penner, J. Phys. Chem. A 108 (2004) 4751.
[44] L. Frydman, J.S. Harwood, J. Am. Chem. Soc. 117 (1995) 5367.
[45] Z. Gan, J. Am. Chem. Soc. 122 (2000) 3242.
[46] H. Trill, H. Eckert, V.I. Srdanov, J. Phys. Chem. B 107 (2003) 8779.
[47] F.H. Larsen, H.J. Jakobsen, P.D. Ellis, N.C. Nielsen, J. Phys. Chem. A 101 (1997) 8597.
[48] D.L. Bryce, G.D. Sward, J. Phys. Chem. B. 110 (2006) 26461.
[49] D.L. Bryce, G.D. Sward, S. Adiga, J. Am. Chem. Soc. 128 (2006) 2121.
[50] R.P. Chapman, D.L. Bryce, Phys. Chem. Chem. Phys. 9 (2007) 6219.
[51] C.M. Widdifield, D.L. Bryce, (unpublished work).
[52] A.J. Rossini, R.W. Mills, G.A. Briscoe, E.L. Norton, S.J. Geier, I. Hung, S. Zheng, J. Autschbach, R.W. Schurko, J. Am. Chem. Soc. 131 (2009) 3317.
[53] D.L. Bryce, M. Gee, R.E. Wasylishen, J. Phys. Chem. A 105 (2001) 10413.
[54] R. Siegel, T.T. Nakashima, R.E. Wasylishen, Concept Magn. Reson. A 26 (2005) 62.
[55] R. Siegel, T.T. Nakashima, R.E. Wasylishen, Concept Magn. Reson. A 26 (2005) 47.
[56] A.P.M. Kentgens, R. Verhagen, Chem. Phys. Lett. 300 (1999) 435.
[57] R. Siegel, T.T. Nakashima, R.E. Wasylishen, Chem. Phys. Lett. 388 (2004) 441.
[58] L.A. O'Dell, R.W. Schurko, Chem. Phys. Lett. 464 (2008) 97.
[59] L.A. O'Dell, A.J. Rossini, R.W. Schurko, Chem. Phys. Lett. 468 (2009) 330.
[60] A. Samoson, Chem. Phys. Lett. 119 (1985) 29.
[61] C. Jäger, Satellite transition spectroscopy of quadrupolar nuclei, in: P. Diehl, E. Fluck, H. Günther, R. Kosfeld, J. Seelig (Eds.), NMR Basic Principles and Progress, vol. 31, Springer-Verlag, Berlin, 1994, pp. 133–170.
[62] J. Skibsted, N.C. Nielsen, H. Bildsøe, H.J. Jakobsen, J. Magn. Reson. 95 (1991) 88.
[63] J. Persons, G.S. Harbison, J. Magn. Reson. 186 (2007) 347.
[64] K. Eichele, R.E. Wasylishen, WSOLIDS NMR Simulation Package 1.17.30, 2001.
[65] D.W. Alderman, M.S. Solum, D.M. Grant, J. Chem. Phys. 84 (1986) 3717.
[66] M. Bak, J.T. Rasmussen, N.C. Nielsen, J. Magn. Reson. 147 (2000) 296.
[67] D. Massiot, F. Fayon, M. Capron, I. King, S. Le Calvé, B. Alonso, J.-O. Durand, B. Bujoli, Z. Gan, G. Hoatson, Magn. Reson. Chem. 40 (2002) 70.
[68] P. Pyykkö, Mol. Phys. 106 (2008) 1965.
[69] S. Hayashi, K. Hayamizu, J. Phys. Chem. Solids 53 (1992) 239.
[70] J. Skibsted, H.J. Jakobsen, Inorg. Chem. 38 (1999) 1806.
[71] T. Kanda, J. Phys. Soc. Jpn. 10 (1955) 85.
[72] Y. Yamagata, J. Phys. Soc. Jpn. 19 (1964) 10.
[73] T.L. Weeding, W.S. Veeman, J. Chem. Soc. Chem. Commun. (1989) 946.
[74] S. Hayashi, K. Hayamizu, Bull. Chem. Soc. Jpn. 63 (1990) 913.
[75] F. Lefebvre, J. Chim. Phys. 89 (1992) 1767.
[76] H. Honda, Z. Naturforsch. 58a (2003) 623.
[77] T. Yamanishi, T. Kanashiro, A. Itabashi, Y. Michihiro, Y. Kishimoto, T. Ohno, J. Phys. Soc. Jpn. 63 (1994) 3903.
[78] T. Yamanishi, T. Kanashiro, Y. Michihiro, Y. Kishimoto, T. Ohno, J. Phys. Soc. Jpn. 64 (1995) 643.
[79] Y. Michihiro, T. Yamanishi, T. Kanashiro, Y. Kishimoto, Solid State Ionics 79 (1995) 40.
[80] T. Kanashiro, Y. Michihiro, K. Kitahara, T. Yamanishi, Y. Kishimoto, T. Ohno, Solid State Ionics 86–88 (1996) 223.
[81] J.L. Marsh Jr., P.A. Casabella, Phys. Rev. 150 (1966) 546.
[82] K. Eichele, R.E. Wasylishen, J.S. Grossert, A.C. Olivieri, J. Phys. Chem. 99 (1995) 10110.
[83] D.L. Bryce, E.B. Bultz, Chem. Eur. J. 13 (2007) 4786.
[84] J.F. Stebbins, L.S. Du, Am. Mineral. 87 (2002) 359.
[85] T.O. Sandland, L.S. Du, J.F. Stebbins, J.D. Webster, Geochem. Cosmochim. Acta 68 (2004) 5059.
[86] J.P. Yesinowski, M.L. Buess, A.N. Garroway, M. Ziegeweld, A. Pines, Anal. Chem. 67 (1995) 2256.
[87] C. Gervais, R. Dupree, K.J. Pike, C. Bonhomme, M. Profeta, C.J. Pickard, F. Mauri, J. Phys. Chem. 109 (2005) 6960.
[88] H. Hamaed, J.M. Pawlowski, B.F.T. Cooper, R. Fu, S.H. Eichhorn, R.W. Schurko, J. Am. Chem. Soc. 130 (2008) 11056.
[89] A. Lupulescu, M. Kotecha, L. Frydman, J. Am. Chem. Soc. 125 (2003) 3376.
[90] P.G. Gordon, D.H. Brouwer, J.A. Ripmeester, J. Phys. Chem. A 112 (2008) 12527.
[91] P.G. Gordon, D.H. Brouwer, J.A. Ripmeester, Probing the local structure of ionic liquid salts with ^{35}Cl, ^{79}Br and ^{127}I solid state NMR. 40th Inorganic Discussion Weekend, University of Toronto, Toronto, 2007, p. 21.
[92] C. Hardacre, S.E.J. Holbrey, J.D. McMath, D.T. Bowron, A.K. Soper, J. Chem. Phys. 118 (2003) 273.
[93] S. Tsuzuki, H. Tokuda, M. Mikami, Phys. Chem. Chem. Phys. 9 (2007) 4780.
[94] H. Katayanagi, S. Hayashi, H. Hamaguchi, K. Nishikawa, Chem. Phys. Lett. 392 (2004) 460.
[95] S. Jurga, J. Seliger, R. Blinc, H.W. Spiess, Phys. Lett. A 116 (1986) 295.
[96] S.L. Segel, S. Maxwell, R.D. Heyding, P. Ingman, E. Ylinen, M. Punkkinen, Solid State Commun. 66 (1988) 1039.
[97] T.J. Bastow, S.N. Stuart, J. Phys. Condens. Matter 1 (1989) 4649.
[98] V.P. Tarasov, M.A. Meladze, G.A. Kirakosyan, A.E. Shvelashvili, Y.A. Buslaev, Phys. Status Solidi B 167 (1991) 271.
[99] V.P. Tarasov, M.A. Meladze, G.A. Kirakosyan, Russ. J. Coord. Chem. 18 (1992) 823.
[100] N. Binesh, S.V. Bhat, Solid State Ionics 92 (1996) 261.
[101] H. Ono, S. Ishimaru, R. Ikeda, H. Ishida, Chem. Phys. Lett. 275 (1997) 485.
[102] H. Ono, S. Ishimaru, R. Ikeda, H. Ishida, Bull. Chem. Soc. Jpn. 72 (1999) 2049.
[103] O. Czupiński, M. Wojtaś, J. Zaleski, R. Jakubas, W. Medycki, J. Phys. Condens. Matter 18 (2006) 3307.
[104] R.V. Pound, Phys. Rev. 79 (1950) 685.
[105] G.D. Watkins, R.V. Pound, Phys. Rev. 89 (1953) 658.
[106] R.V. Pound, J. Phys. Chem. 57 (1953) 743.
[107] M.J. Weber, Phys. Rev. 130 (1963) 1.
[108] R.R. Allen, M.J. Weber, J. Chem. Phys. 38 (1963) 2970.
[109] M.J. Weber, R.R. Allen, Proc. Coll. AMPERE 11 (1963) 177.
[110] B.D. Günther, M.L. Simon, R.A. Hultsch, B. Am. Phys. Soc. Ser. 2 (14) (1969) 188.
[111] T.C. Ng, E. Tward, J. Magn. Reson. 51 (1983) 361.
[112] F. Reif, Phys. Rev. 100 (1955) 1597.
[113] E. Otsuka, H. Kawamura, J. Phys. Soc. Jpn. 12 (1957) 1071.
[114] M.E. Melich, W.D. Ohlsen, B. Am. Phys. Soc. Ser. 2 (8) (1963) 468.
[115] W.D. Ohlsen, M.E. Melich, Phys. Rev. 144 (1966) 240.
[116] K.D. Becker, J. Phys.-Paris, Colloque 41 (1980) C6–249.
[117] O.A.P. Tavares, B. D'Aguanno, L.G. Conti, Gazz. Chim. Ital. 113 (1983) 529.
[118] J.S. Frye, G.E. Maciel, J. Magn. Reson. 48 (1982) 125.
[119] K.R. Thurber, R. Tycko, J. Magn. Reson. 196 (2009) 84.
[120] B.H. Suits, D. White, J. Appl. Phys. 60 (1986) 3772.
[121] V.P. Tarasov, S.A. Petrushin, Y.K. Gusev, Dokl. Akad. Nauk SSSR 293 (1987) 1423.

[122] T. Erge, D. Michel, J. Petersson, F. Engelke, Phys. Status Solidi A 123 (1991) 325.
[123] D.M. Potrepka, J.I. Budnick, D.B. Fenner, W.A. Hines, M. Balasubramanian, A.R. Moodenbaugh, Phys. Rev. B 60 (1999) 10489.
[124] H. Trill, H. Eckert, V.I. Srdanov, J. Am. Chem. Soc. 124 (2002) 8361.
[125] K.D. Becker, E. von Goldammer, Chem. Phys. 48 (1980) 193.
[126] S.L. Segel, H.M. Vyas, J. Chem. Phys. 72 (1980) 1406.
[127] G. Wu, S. Dong, Solid State Nucl. Magn. Reson. 20 (2001) 100.
[128] P.K. Burkert, Z. Naturforsch. 35b (1980) 1349.
[129] J.F. Hon, K.O. Christe, J. Chem. Phys. 52 (1970) 1960.
[130] R. Fusaro, J.W. Doane, J. Chem. Phys. 47 (1967) 5446.
[131] X. Hou, R.J. Kirkpatrick, Inorg. Chem. 40 (2001) 6397.
[132] X. Hou, A.G. Kalinichev, R.J. Kirkpatrick, Chem. Mater. 14 (2002) 2078.
[133] X. Hou, R.J. Kirkpatrick, Chem. Mater. 14 (2002) 1195.
[134] R.B. Creel, E. von Meerwall, C.F. Griffin, R.G. Barnes, J. Chem. Phys. 58 (1973) 4930.
[135] A. Kawamori, J. Itoh, J. Phys. Soc. Jpn. 18 (1963) 1614.
[136] F. Tabak, A. Lascialfari, A. Rigamonti, J. Phys Conden. Matter 5 (1993) B31.
[137] H.W. Spiess, R.K. Sheline, J. Chem. Phys. 54 (1971) 1099.
[138] R.G. Barnes, S.L. Segel, J. Chem. Phys. 37 (1962) 1895.
[139] W.H. Jones, S.L. Segel, Phys. Rev. Lett. 13 (1964) 528.
[140] S.H. Choh, C.V. Stager, Can. J. Phys. 49 (1971) 144.
[141] T.J. Bastow, S.N. Stuart, W.G. McDugle, R.S. Eachus, J.M. Spaeth, J. Phys. Condens. Matter 6 (1994) 8633.
[142] C. Brinkmann, S. Faske, M. Vogel, T. Nilges, A. Heuer, H. Eckert, Phys. Chem. Chem. Phys. 8 (2006) 369.
[143] M. Hattori, Y. Onoda, T. Erata, M.E. Smith, M. Hattori, H. Ohki, R. Ikeda, Z. Naturforsch. 49a (1994) 291.
[144] K. Saito, K. Kanehashi, I. Komaki, Annu. Rep. Nucl. Magn. Reson. Spectrosc. 44 (2001) 23.
[145] S. Mulla-Osman, D. Michel, Z. Czapla, W.D. Hoffman, J. Phys. Condens. Matter 10 (1998) 2465.
[146] S. Mulla-Osman, D. Michel, G. Völkel, Z. Czapla, Phys. Status Solidi B 219 (2000) 9.
[147] S. Mulla-Osman, D. Michel, G. Völkel, I. Peral, G. Madariaga, J. Phys. Condens. Matter 13 (2001) 1119.
[148] S.D. Goren, L.F. Ben-Yakar, A. Shames, B. Pandyopadhayay, C. Korn, H. Shaked, P. Massiot, C. Perrin, J. Gallier, A. Privalov, Physica C 313 (1999) 127.
[149] R.J. Kirkpatrick, P. Yu, X. Hou, Y. Kim, Am. Mineral. 84 (1999) 1186.
[150] K. Yamada, K. Isobe, T. Okuda, Y. Furukawa, Z. Naturforsch. 49a (1994) 258.
[151] K. Yamada, K. Isobe, E. Tsuyama, T. Okuda, Y. Furukawa, Solid State Ionics 79 (1995) 152.
[152] E.B. Amitin, N.V. Bausck, S.A. Gromilov, S.G. Kozlova, N.K. Moroz, L.N. Mazalov, V.N. Naumov, P.P. Samoilov, S.A. Slobodjan, M.A. Starikov, V.E. Fedorov, G.I. Frolova, S.B. Erenburg, Physica C 209 (1993) 407.
[153] J.P. Yesinowski, H. Eckert, Unpublished data, 1985.
[154] F.M. McCubbin, H.E. Mason, H. Park, B.L. Phillips, J.B. Parise, H. Nekvasil, D.H. Lindsley, Am. Mineral. 93 (2008) 210.
[155] T. Saito, H. Inoue, J. Tonisi, A. Oosawa, T. Goto, T. Sasaki, N. Kobayasi, S. Awaji, K. Watanabe, J. Phys. Conf. Ser. 51 (2006) 203.
[156] F. Barberon, V. Baroghel-Bouny, H. Zanni, B. Bresson, J.B. d'Espinose de la Caillerie, L. Malosse, Z. Gan, Magn. Reson. Imaging 23 (2005) 267.
[157] B.D. Günther, R.A. Hultsch, J. Magn. Reson. 1 (1969) 609.
[158] R. Jelinek, A. Stein, G.A. Ozin, J. Am. Chem. Soc. 115 (1993) 2390.
[159] J. Itoh, Y. Yamagata, J. Chem. Phys. 24 (1956) 621.
[160] J. Itoh, Y. Yamagata, J. Phys. Soc. Jpn. 17 (1962) 481.
[161] K.R. Jeffrey, A.G. Brown, R.L. Armstrong, Phys. Rev. B 8 (1973) 3071.
[162] S. Hayashi, K. Hayamizu, J. Chem. Phys. 92 (1990) 2818.
[163] V.P. Tarasov, V.I. Privalov, K.S. Gavrichev, V.E. Gorbunov, Y.K. Gusev, Y.A. Buslaev, Russ. J. Coord. Chem. 16 (1990) 854.
[164] V.P. Tarasov, S.A. Petrushin, Y.K. Gusev, Russ. J. Inorg. Chem. 33 (1988) 452.
[165] R. Jelinek, B.F. Chmelka, A. Stein, G.A. Ozin, Multinuclear solid-state NMR study of a sodalite semiconductor supralattice. Mater. Res. Soc. Symp. Proc., San Francisco, California, USA, 1992, p. 235.
[166] P. Brenni, D. Brinkmann, H. Huber, M. Mali, J. Roos, H. Arend, Solid State Commun. 47 (1983) 415.
[167] D. Brinkmann, H. Huber, M. Mali, J. Roos, H. Arend, Helv. Phys. Acta 55 (1982) 568.
[168] H. Nakayama, T. Eguchi, N. Nakamura, H. Chihara, T. Nogami, K. Imamura, Y. Shirota, Bull. Chem. Soc. Jpn. 62 (1989) 399.
[169] F. Milia, G. Papavassiliou, A. Leventis, G. Papantopoulos, P. Venturini, D. Mihailovic, J. Pirnat, R. Blinc, Br NMR study of $C_{60}Br_{24}Br_2$. Proceedings of the International Winterschool on Electronic Properties of Novel Materials, Kirchber, Austria, 1995, pp. 470–473.
[170] F. Milia, G. Papavassiliou, A. Leventis, J. Dolinsek, ^{13}C and ^{81}Br NMR in $C_{60}Br_{24}Br_2$. Proceedings of the International Winterschool on Electronic Properties of Novel Materials, Kirchberg, Austria, 1995, p. 159.
[171] A. Kehrer, N. Weiden, A. Weiss, Z. Phys. Chem. 178 (1992) 1.
[172] M. Grommelt, P.K. Burkert, Z. Naturforsch. 44b (1989) 1053.
[173] D.G. Klobasa, P.K. Burkert, Z. Naturforsch. 42a (1987) 275.
[174] D.G. Klobasa, P.K. Burkert, G. Müller, Z. Naturforsch. 41a (1986) 330.
[175] P.K. Burkert, D.G. Klobasa, Z. Naturforsch. 40a (1985) 274.
[176] J.M. Weulersse, J. Virlet, P. Rigny, Mol. Phys. 38 (1979) 923.
[177] R.K. Harris, E.D. Becker, S.M. Cabral De Menezes, P. Granger, R.E. Hoffman, K.W. Zilm, Pure Appl. Chem. 80 (2008) 59.